



# Pacific superplume-related oceanic basalts hosted by accretionary complexes of Central Asia, Russian Far East and Japan

I. Yu. Safonova <sup>a,\*</sup>, A. Utsunomiya <sup>b</sup>, S. Kojima <sup>c</sup>, S. Nakae <sup>d</sup>, O. Tomurtogoo <sup>e</sup>, A.N. Filippov <sup>f</sup>, K. Koizumi <sup>g</sup>

<sup>a</sup> Institute of Geology and Mineralogy, SB RAS, Novosibirsk 630090, Russia

<sup>b</sup> Institute of Earth Sciences, Academia Sinica, Taipei 11529, Taiwan

<sup>c</sup> Department of Civil Engineering, Gifu University, Gifu 501-1193, Japan

<sup>d</sup> Geological Survey of Japan, AIST, Tsukuba 305-8567, Japan

<sup>e</sup> Institute of Geology and Mineral Resources, MAS, Ulaanbaatar 210357, Mongolia

<sup>f</sup> Far-East Geological Institute, FEB RAS, Vladivostok 690022, Russia

<sup>g</sup> Society of Gem and Precious Metal, Kofu-city, 400-0055, Japan

## ARTICLE INFO

### Article history:

Received 30 October 2008

Received in revised form 16 February 2009

Accepted 20 February 2009

Available online 9 March 2009

### Keywords:

Paleo-Asian Ocean

Paleo-Pacific Ocean

Evolution

Intraplate magmatism

Trace-element composition

Oceanic plate stratigraphy

## ABSTRACT

Plume-related oceanic magmatism form oceanic islands, seamounts and plateaus (hereafter “seamounts” or “paleoseamounts”), which are important features in geological history. The accretion of oceanic seamounts to active continental margins significantly contributed to the formation of the continental crust. This paper reviews occurrences of Late Neoproterozoic–Mesozoic seamounts of the Paleo-Asian and Paleo-Pacific oceans, which are hosted by accretionary complexes (ACs) of Russian Altai, East Kazakhstan, Mongolia, Russian Far East and Japan. The paleoseamounts commonly consist of Ti–LREE–Nb-enriched plume-related basalts (OIB-type or intraplate basalts) capped with massive limestone and associated with other units of oceanic plate stratigraphy (OPS): oceanic floor basalts (MORB), pelagic chert, epiclastic slope facies, etc. The paper presents available geochemical data on the plume-related basalts including the first geochemical data on the Middle Paleozoic OIB-type basalts of the Paleo-Asian Ocean hosted by the Ulaanbaatar AC of Mongolia. An emphasis is made for the structural setting of OPS units, specific geochemical features of intraplate basalts, problems of their identification, and distinguishing from magmatic units of a different origin such as MORB, island-arc and back-arc basalts. Finally, we propose a continuous, though periodical, evolution of the Pacific superplume-related magmatism, which can be more reliably proved by studying Middle Paleozoic OPS units hosted by ACs of Mongolia and Tien Shan, and discuss prospects of future studies.

© 2009 International Association for Gondwana Research. Published by Elsevier B.V. All rights reserved.

## 1. Introduction

Basaltic oceanic islands, seamounts and plateaus are important features in geological history. They record specific magmatism related to the action of mantle plumes and superplumes. Mantle plumes, columns of heated material ascending from the lower mantle, are expressed on the surface as hot spots (e.g., Hofmann, 1997). Hot spot magmatism produced oceanic islands and seamounts like those of the Hawaii Islands and Emperor-Hawaii Seamount Chain (e.g. Regelous et al., 2003 and there references cited therein). Superplumes are giant mantle plumes or upwellings probably derived from the core–mantle boundary (Maruyama, 1994; Maruyama et al., 2007). They are thought to be responsible for such globally important geological events as breakup of continents, opening of oceans (Maruyama, 1994) and extensive volcanic eruptions, forming large igneous provinces (LIPs) on continents, e.g. the Permian–Triassic flood basalts or traps in East Siberia (e.g., Medvedev et al., 2003; Reichow et al., 2009), or huge

basaltic plateaus in oceans, like the Mid-Cretaceous plateau basalts in the western Pacific (e.g., Mahoney et al., 1993; Neal et al., 1997). Both the plume- and superplume-related volcanism events are believed to have affected the global environment. The proposed superplume-related volcanism events at the Vendian–Cambrian, Permo-Triassic boundaries and during the mid-Cretaceous pulse are considered to have resulted in mass extinction of biota (e.g., Kerr, 1998; Wignall, 2001; Utsunomiya et al., 2008; Reichow et al., 2009). Mantle plumes and superplumes seem to be mutually related: a superplume can split into separate plumes near the Moho boundary as has been suggested for the Pacific Superplume (Maruyama et al., 2007).

According to different opinions the Pacific Superplume developed at around 750–600 Ma and broke up the Rodinia Supercontinent to give birth to the Paleo-Pacific Ocean (Maruyama, 1994; Condie, 2003; Maruyama et al., 2007; Santosh et al., 2009a,b). Dobretsov et al. (2003) argued that there were two stages of the Rodinia breakup in response to the initiation of the Superplume: the first stage at 970–850 Ma opened the Paleo-Asian Ocean and the second stage at 750–700 Ma resulted in the opening of the Paleo-Pacific. After the opening of paleo-oceans the Pacific Superplume caused intraplate oceanic

\* Corresponding author.

E-mail address: [inna@uiggm.nsc.ru](mailto:inna@uiggm.nsc.ru) (I.Y. Safonova).

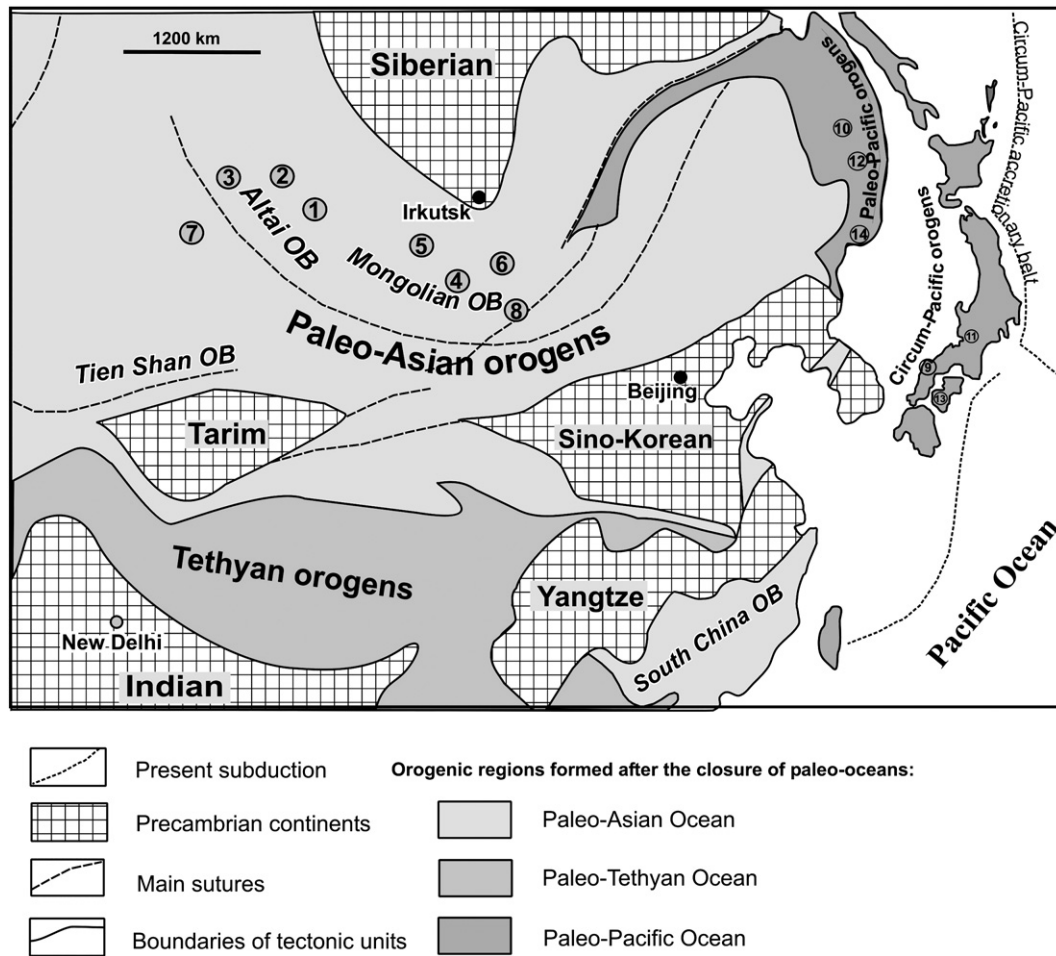


**Fig. 1.** Simplified tectonic scheme of Asia showing the main orogens formed after the closure of paleo-oceans (modified from Ren et al., 1999). Approximate location of local orogenic belts (OB) and accretionary complexes (numbers in circles, in decreasing order of age): 1 – Kurai, 2 – Katun, 3 – Zasur'ya, 4 – Bayanhongor, 5 – Agardag, 6 – Ulaanbaatar, 7 – Char, 8 – Solonker, 9 – Akiyoshi, 10 – Khabarovsk, 11 – Mino–Tamba, 12 – Samarka, 13 – Chichibu, 14 – Taukha.

magmatism: more local hotspot volcanism formed oceanic islands/seamounts and more extensive volcanism formed larger oceanic plateaus. Later, oceanic island and oceanic plateau basalts (OIB and OPB, respectively) were accreted to continental margins during subduction and closure of the paleo-oceans (e.g., Maruyama et al., 1997; Buslov et al., 2001; Utsunomiya et al., 2007). Remnants of former oceanic islands/plateaus formed in the Paleo-Asian and Paleo-Pacific Oceans, PAO and PPO, respectively, (Fig. 1) are presently hosted by accretionary complexes of Central Asia (e.g., Buslov et al., 2001, 2004a; Windley et al., 2007; Yakubchuk, 2004), Russian Far East (e.g. Khanchuk et al., 1989b; Kojima et al., 2000; Kemkin, 2006) and Japan and surrounding regions (e.g., Isozaki et al., 1990; Maruyama et al., 1997; Kojima et al., 2000; see also Hara et al. 2009 for Paleo-Tethys). The intraplate or OIB-type basalts are usually enriched in incompatible elements and represent parts of oceanic plate stratigraphy (OPS), which also includes typical oceanic sediments: pelagic radiolarian/ribbon chert, hemipelagic siliceous shale, mudstone and other epiclastic slope facies and shallow-water limestone or carbonate “cap” (Isozaki et al., 1990).

Previously identified accreted OPS units of two oceans were thought to be formed during two main periods: Late Neoproterozoic–Early Paleozoic and Late Paleozoic–Mesozoic with a Middle Paleozoic hiatus, first identified by Safonova (2009). The Late Neoproterozoic–Early Paleozoic stage of the plume-related or intraplate oceanic magmatism of the Paleo-Asian Ocean is recorded by OIB-type basaltic lavas and their associated OPS units, incorporated into accretionary complexes of the Central Asian Orogenic Belt: Kurai (Late Neoproterozoic; Russian Gorny

Altai), Bayanhongor (Late Neoproterozoic; Central Mongolia), Katun (Early Cambrian; Russian Gorny Altai) and Zasur'ya (Late Cambrian; NE Russian Altai). The Late Paleozoic stage of the Paleo-Asian Ocean intraplate magmatism is recorded in the Char AC of East Kazakhstan (Early Carboniferous) and Solonker AC of SE Mongolia–North China (Late Carboniferous). This paper presents new data on the Middle Paleozoic plume-related OPS units hosted by the Ulaanbaatar AC (Late Silurian–Early Devonian; northern Mongolia).

In the Paleo-Pacific Ocean, the OIB- and OPB-type basalts were formed during a long period from the Late Paleozoic until the Late Mesozoic and later were incorporated in accretionary complexes of Russian Far East and their analogues in Central and SW Japan, respectively: the lower part of the Khabarovsk AC and the Akiyoshi AC (Late Carboniferous–Permian), Samarka and Mino–Tamba ACs (Permian–Triassic), Taukha and Southern Chichibu ACs (Jurassic; Fig. 1). In Cretaceous time, the Pacific superplume-related volcanism continued in the Pacific oceanic realm (Maruyama et al., 2007) and formed the Emperor Seamount Chain, which oldest fragments are hosted by accretionary complexes of East Kamchatka (Saveliev, 2003; Shapiro et al., 2007).

The aim of this paper is to review accretionary complexes of Central and Far East Asia hosting OPS units with intraplate basalts of the Paleo-Asian and Paleo-Pacific oceans (Fig. 1; Table 1), which formed due to the activity of the Pacific Superplume and its related local mantle plumes (Maruyama et al., 2007). The paper presents both published and original geochemical data on those basalts to evaluate the current models for their origin and to enable conclusions about the evolution of plume-related magmatism of the two oceans. We will

**Table 1**

Accretionary complexes and their hosted plume-related basalts of the Paleo-Asian and Paleo-Pacific Oceans: location, age, geodynamic stage.

Accretionary complex (no. in figures)	Geographic location	Age and name of associated OPS units; Isotope geochronology (where available)	Age of accretion and geodynamic stage
<i>Paleo-Asian Ocean</i>			
Kurai (1)	Southern Gorny Altai, Russian Altai	Ediacaran stromatolite and microphytolite; <i>Baratal Fm.</i> (Buslov et al., 1993) 598 ± 25 Ma; Pb–Pb dating of carbonates (Uchio et al., 2004)	Early–Middle Cambrian accretion of the paleoseamounts and Kuznetsk–Altai island arc to the SE margin of the Siberian continent (Buslov et al., 2001; Dobretsov et al., 2004; Safonova et al., 2004)
Katun (2)	Northern Gorny Altai	Early Cambrian algae and sponge spicules; <i>Manzherok Fm.</i> (Terleev, 1991)	
Agardag (5)	Northwestern Mongolia	Sm–Nd isochron, 570 ± 1 Ma (Pfander et al., 1998)	Accretion of an island-arc (Badarch et al., 2002) or Red Sea-type rifting (Dobretsov et al., 2005)
Bayanhongor (4)	Central Mongolia	Early Cambrian brachiopods (Ryazantsev, 1994) Sm–Nd isochron, 569 ± 21 Ma (Kepezhinskas et al., 1991)	Collision of the Baydrag cratonic block and Orhon terrain of Late Cambrian age (Kovalenko et al., 2005)
Zasur'ya (3)	Rudny Altai, Northeastern Russian Altai	Late Cambrian–Early Ordovician conodonts, radiolarians and sponge spicules; <i>Zasur'ya Series</i> (Iwata et al., 1997b; Sennikov et al., 2003)	Late Ordovician–Early Devonian accretion of seamounts to the Altai–Mongolian microcontinent (Buslov et al., 2001, 2004b; Safonova et al., 2004)
Ulanbaatar (6)	Northern Mongolia	Late Silurian–Late Devonian conodonts and radiolarians; <i>Gorkhi Fm.</i> (Kashiwagi et al., 2004)	No distinct geodynamic model available; probably Carboniferous accretion of oceanic islands to an active margin of the Siberian continent (Parfenov et al., 1995)
Char (7)	East Kazakhstan	Late Devonian–Early Carboniferous radiolarians and conodonts; <i>Karabaev and Urumbaev Fms.</i> (Iwata et al., 1997a; Sennikov et al., 2003)	Late Carboniferous–Permian accretion of oceanic islands to the Siberian continent active margin (Buslov et al., 2004a,b; Safonova et al., 2004)
Solonker (8)	Southeastern Mongolia–China border	Lower Permian fusulinids and Upper Permian brachiopods and bryozans in limestones; <i>Boroinsul Fm.</i> (Pavlova et al., 1991)	The Late Permian collision of the North China craton active margin and South Mongolian active margin of the Siberian craton and closure of the Paleo-Asian ocean (Xiao et al., 2003; Windley et al., 2007)
<i>Paleo-Pacific Ocean</i>			
Khabarovsk (lower part) (10)	Central Sikhote-Alin, Russian Far East	Carboniferous–Permian fusulinids and conodonts, <i>Khabarovsk Fm.</i> (Shevelev, 1987; Suzuki et al., 2005)	Early Permian subduction of the Farallon Plate beneath the Yangtze Block and accretion of seamounts to the southern margin of the Yangtze block (Kanmera et al., 1990; Maruyama et al., 1997)
Akiyoshi (9)	Southwestern Japan	Middle Carboniferous–Permian fusulinids, conodonts and radiolarians, <i>Akiyoshi and Nishiki Groups</i> , (Isozaki et al., 1990; Isozaki, 1997)	
Samarka (12)	Central and southern Sikhote-Alin	Carboniferous and Permian radiolarians, fusulinaceans and algae; <i>Sebuchar Fm.</i> (Belyanskiy et al., 1984; Khanchuk et al., 1989a)	Early–Middle Jurassic orthogonal subduction of the Izanagi Plate beneath amalgamated Asia and Middle Jurassic accretion of seamounts to East Asia (Isozaki, 1997; Maruyama et al., 1997)
Mino-Tamba (11)	Central Japan	Middle–Late Permian radiolarians; <i>Kozuki Fm.</i> (Pillai and Ishiga, 1987)	
Taukha (14)	Southeastern Sikhote-Alin	Jurassic (Callovian) to Cretaceous (Berrisian) radiolarians; <i>Erdagous Fm.</i> , <i>Gorbusha S.</i> (Golozubov et al., 1992)	Early Cretaceous oblique subduction of the Izanagi Plate beneath East Asia and accretion of the plateau to the East Asia active margin (Maruyama et al., 1997)
Southern Chichibu (13)	Southeastern Japan	Late Jurassic radiolarians and conodonts, <i>Sambosan Fm.</i> (Matsuoka, Yao, 1990)	
<i>Pacific Ocean</i>			
Smagin (15)	East Kamchatka	Early Cretaceous (Albian–Cenomanian; ca 110–100 Ma) radiolarians in chert; <i>Smagin Fm.</i> (Zinkevich et al., 1985)	Miocene accretion of the paleoseamount and Kronotsky island arc to the NE Asia margin (Khotin and Shapiro, 2006)

distinguish main periods of plume-related magmatism and discuss the structural position of basalts and OPS sediments, key geochemical features of intraplate basalts and episodic or continuous character of plume-related magmatism. Emphasis will be given to the problem of their identification in structurally complicated orogenic belts. Proposals for future studies will also be outlined. As a part of this study we report the first occurrence of Middle Paleozoic intraplate oceanic basalts in Central Asia and pioneer in discussing their geochemical features.

The study of intraplate magmatism and associated OPS is very important because it is an integral part of the study of orogenic belts incorporating many commercially valuable mineral deposits. The age and composition of intraplate basalts is necessary for reconstructing the histories of the paleo-oceans and their related accretionary processes, which significantly contributed to the Paleozoic continental growth of Central and East Asia. Last but not least, identification of OIB-type basalts is important for mantle plume modeling and global geodynamic paleoreconstructions.

## 2. Age, occurrence and structure of plume-related basalts

Table 1 summarizes geographic and geological information of the objectives of this study including the location of accretionary

complexes hosting OIB-type basalts, the age of OPS units and methods in its determination and the main geodynamic stages of their accretion to active continental margins.

### 2.1. Late Neoproterozoic–Early Paleozoic

During the Late Neoproterozoic and Early Paleozoic intraplate magmatism was active in the Paleo-Asian Ocean, which, based on the paleoreconstructions by Zonenshain et al. (1990), Dalziel (1992), Dobretsov et al. (1995), was located between the Siberian continent and Western Gondwana and probably reached 4000 km in width. The 600–500 Ma period of major opening of the Paleo-Asian Ocean was characterized by plume-related hot spot magmatism, which formed oceanic islands, seamounts and plateaus (Buslov et al., 2001; Utsunomiya et al., 2007; Safonova, 2009). These oceanic formations were amalgamated with the SW active margin of the Siberian continent (present coordinates) during several stages of subduction, accretion and collision (Fig. 2b). Their fragments presently occur in accretionary complexes of Russian Altai and Central Mongolia.

#### 2.1.1. Russian Altai

The plume-related basaltic units of Late Neoproterozoic, Early Cambrian and Late Cambrian ages have been identified in accretionary

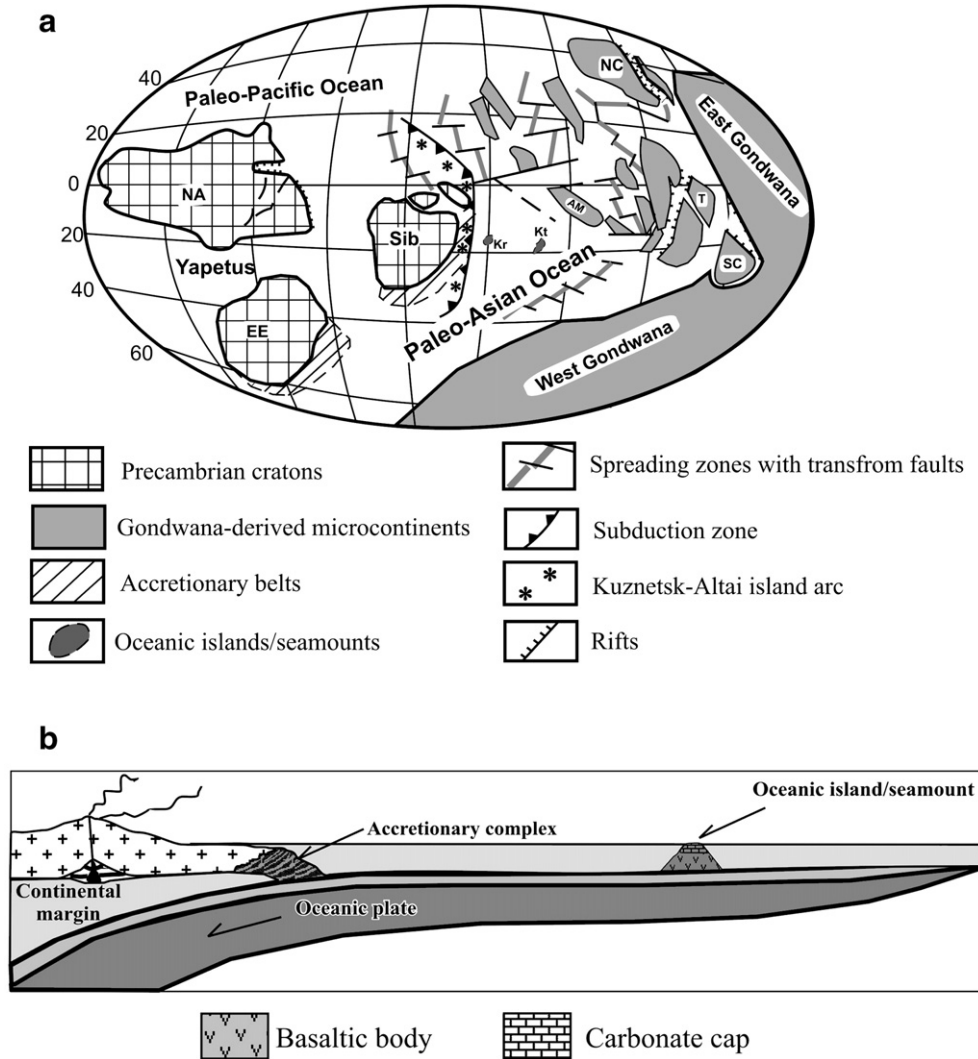


**Fig. 2.** a – Late Neoproterozoic–Cambrian reconstruction of the Paleo-Asian Ocean with paleoseamounts and an island-arc (modified from Kurenkov et al., 2002; Dobretsov et al., 2003). Continental blocks: NA – North America, EE – East Europe, Sib – Siberia, AM – Altai–Mongolian, T – Tarim, NC – North China, SC – South China. Paleoseamounts: Kr – Kurai, Kt – Katun. b – simplified tectonic cartoon showing how oceanic islands/seamounts are accreted to the continental margin.

complexes of Gorny (“mountainous”) and Rudny (“ore”) Altai, Southwest Siberia (Fig. 3). The Kurai and Katun ACs of Gorny Altai host the Kurai and Katun paleoseamounts of Late Neoproterozoic and Early Cambrian ages, respectively (Table 1). Both paleoseamounts (nos. 1 and 2 in Fig. 1) consist of basaltic pillow lavas and dikes and their associated OPS sediments: reefal limestone and deeper marine sediments possessing characteristic features of their formation on oceanic islands slopes such as synsedimentary (asymmetric or intraformational) folding and brecciation (Ota et al., 2007; Safonova, 2008; Safonova et al., 2008).

The Late Cambrian oceanic island units of the Zasukh Series or AC located in Rudny (northwestern) Altai were probably accreted to the active margin of the Gondwana-derived Altai–Mongolian microcontinent before its Devonian collision with the Siberian continent (Table 1; Buslov et al., 2000). The Zasukh Series (no. 3, Fig. 1) includes OIB-type basalts and Late Cambrian–Early Ordovician pelagic cherts (Table 1). It occurs within the Charysh–Terekta shear (strike-slip) zone separating the units of the Siberian continent and Gondwana-derived Altai–Mongolian microcontinent (Fig. 3; Buslov et al., 2000, 2001). The sediments, sandstones and cherts, have brecciated and asymmetrically folded textures (Iwata et al., 1997b; Sennikov et al., 2003). No carbonates have ever been found in the Zasukh Series.

### 2.1.2. Mongolia

Late Neoproterozoic–Cambrian OPS units including intraplate basalts have been identified within the Agardag island-arc terrane (northwestern Mongolia) and Bayanhongor accretionary terrane (Central Mongolia) after the subdivision by Badarch et al. (2002; Fig. 4). However, detailed geochemical data on the oceanic basalts from these areas are very limited. Major element compositions of Bayanhongor basalts were reported in Kopteva et al. (1984) and Ryazantsev (1994). The detailed geochemical study of the Agardag ophiolites, including geochemically variable basalts, has been performed by Pfander et al. (2002).

The Bayanhongor ophiolite terrane or AC (no. 4, Fig. 1) is located on the SW margin of the Hangay Upland (Fig. 4). The generalized ophiolitic section of this complex comprises serpentized peridotite, cumulate sequence, sheeted dikes and Neoproterozoic–Early Cambrian gabbro and pillow lavas (for age details see Table 1). The pillow basalts and gabbro are associated with limestone, siliceous shale and sandstone (Badarch et al., 2002). OIB and OPB-type basalts within the Bayanhongor AC were reported by several researchers (Kepezzhinskas et al., 1991; Kovach et al., 2005; Kovalenko et al., 2005; Tomurhuu and Munkh-Erdene, 2006), who suggested their formation by mantle plume processes. The Bayanhongor AC was formed during the



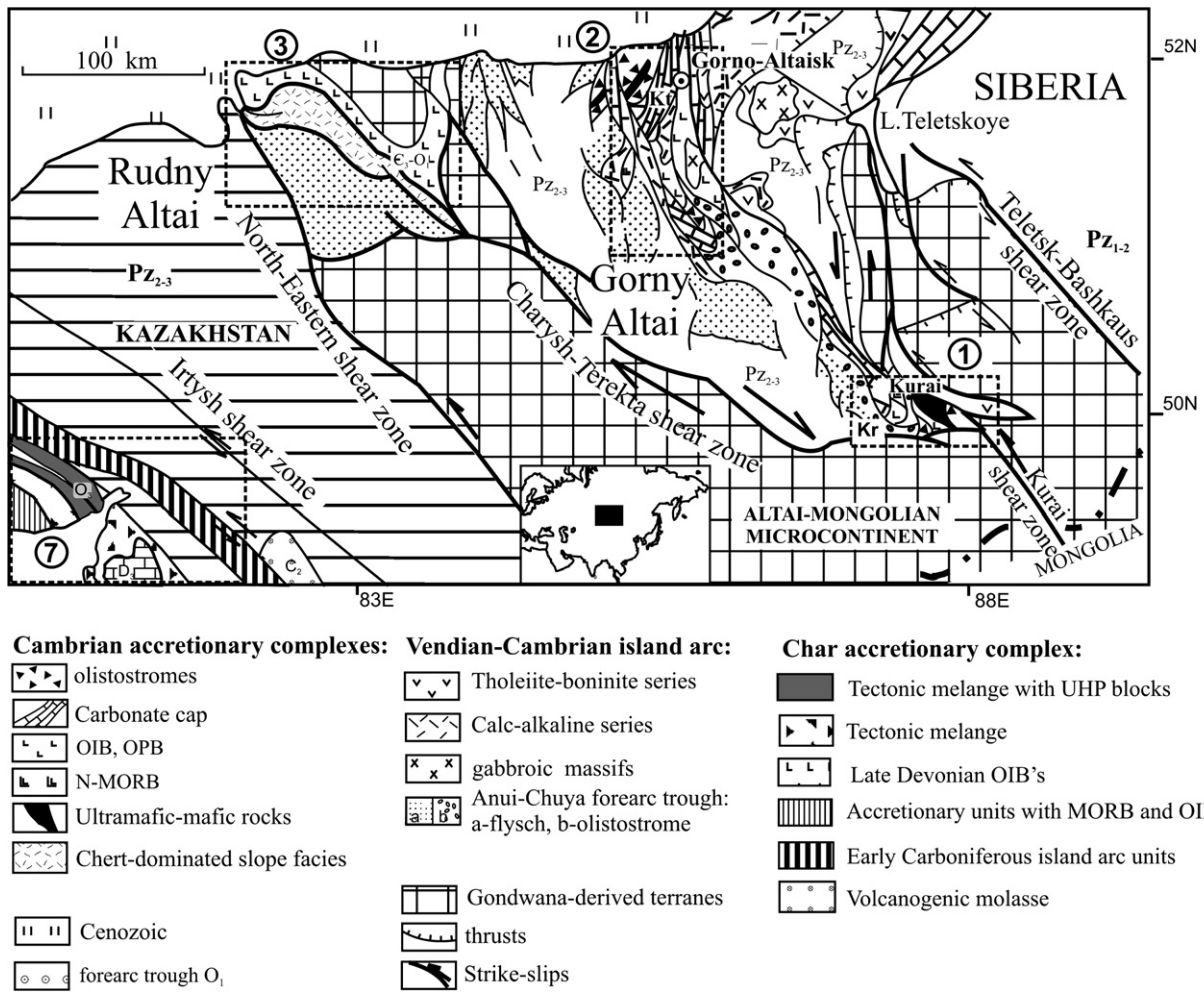


**Fig. 3.** Location and regional geology of accretionary complexes in Gorny Altai (1 – Kurai, 2 – Katun), Northwestern Altai (3 – Zasur'ya) and Eastern Kazakhstan (7 – Char). Locations of ACs are outlined by dashed quadrangles. Well preserved paleoseamounts: Kr – Kurai, Kt – Katun. Modified from Safonova et al. (2004).

collision of the Baidrag cratonic block and Orhon terrain of Late Cambrian age (Kovalenko et al., 2005).

The Agardag terrane (no. 5 in Fig. 1) is located east of Lake Uvs (Fig. 4) and consists of Late Neoproterozoic ophiolites (Table 1) embedded within a tectonic mélangé. The mélangé unit includes mafic schists, basaltic rocks, pillow lavas and typical OPS carbonates and cherts (Pfander et al., 2002). Pfander et al. (2000) and Badarch et al. (2002) regard the Agardag terrane as an island-arc/back-arc terrane, whereas Dobretsov et al. (2005) suggest its riftogenic nature (Red Sea type) possibly indicative of the opening of a paleo-oceanic basin. Parfenov et al. (2006) similarly believe that the Agardag terrane has an oceanic origin. Although, the Ti–LREE–Nb-enriched basalts of the Agardag ophiolites are more often interpreted as island-arc units (Pfander et al., 2002) we believe that at least a part of them could have been formed in an oceanic island setting (see Sections 4 and 5).

**2.2. Middle Paleozoic**

The only occurrence of Middle Paleozoic plume-related oceanic basalts of the Paleo-Asian Ocean has been found in the Ulaanbaatar terrane or AC of northern Mongolia (no. 6; Fig. 1). The Ulaanbaatar AC is located within the Hangay–Hentey basin, between the Aspalt-Hairhan terrane (after Tsukada et al., 2006) or Haraa back-arc terrane (after Badarch et al., 2002) to the NW, Tsetserleg sedimentary terrane to the SW and Adatsag accretionary terrane to the east (Fig. 4). OIB-type basalts have been found in the Gorkhi Formation, which consists of typical OPS sediments: basalt/dolerite, radiolarian chert, siliceous

shale, mudstone, sandstone and limestone (Minjin et al., 2006). The age of the cherts associated with the basalts is constrained from Late Silurian–Late Devonian conodonts and radiolarians (Kurihara et al., 2006). The plume nature of these basalts was initially only briefly discussed by Tsukada et al. (2006). In this paper we present further evidence of the plume-related formation of these basalts, with the results from their first major and trace-element compositional analysis (Section 4).

**2.3. Late Paleozoic–Mesozoic**

**2.3.1. Paleo-Asian Ocean**

The Late Paleozoic was the time of closure of the Paleo-Asian Ocean: its eastern segment closed in the Late Carboniferous–Early Permian (Dobretsov et al., 1995; Xiao et al., 2003), whereas its western part closed in the Late Ordovician (Buslov et al., 2004b). The fragments of Carboniferous oceanic islands were incorporated in the Char AC of East Kazakhstan and Solonker AC at the SE Mongolia–NW China border (Figs. 1, 3 and 4; Table 1).

The Char ophiolitic belt or AC (no. 7, Fig. 1), together with an Early Carboniferous island-arc complex (Buslov et al., 2004b) separates the units of the Kazakhstan and Siberian continents (Fig. 3). It hosts the Late Devonian–Early Carboniferous oceanic island basalts, which were probably formed in the NE branch of the PAO and accreted to the active margin of the Siberian continent during its closure in Late Carboniferous time as a result of Siberia–Kazakhstan collision (Table 1; Buslov et al., 2001). The OIB-type units occur as tectonic

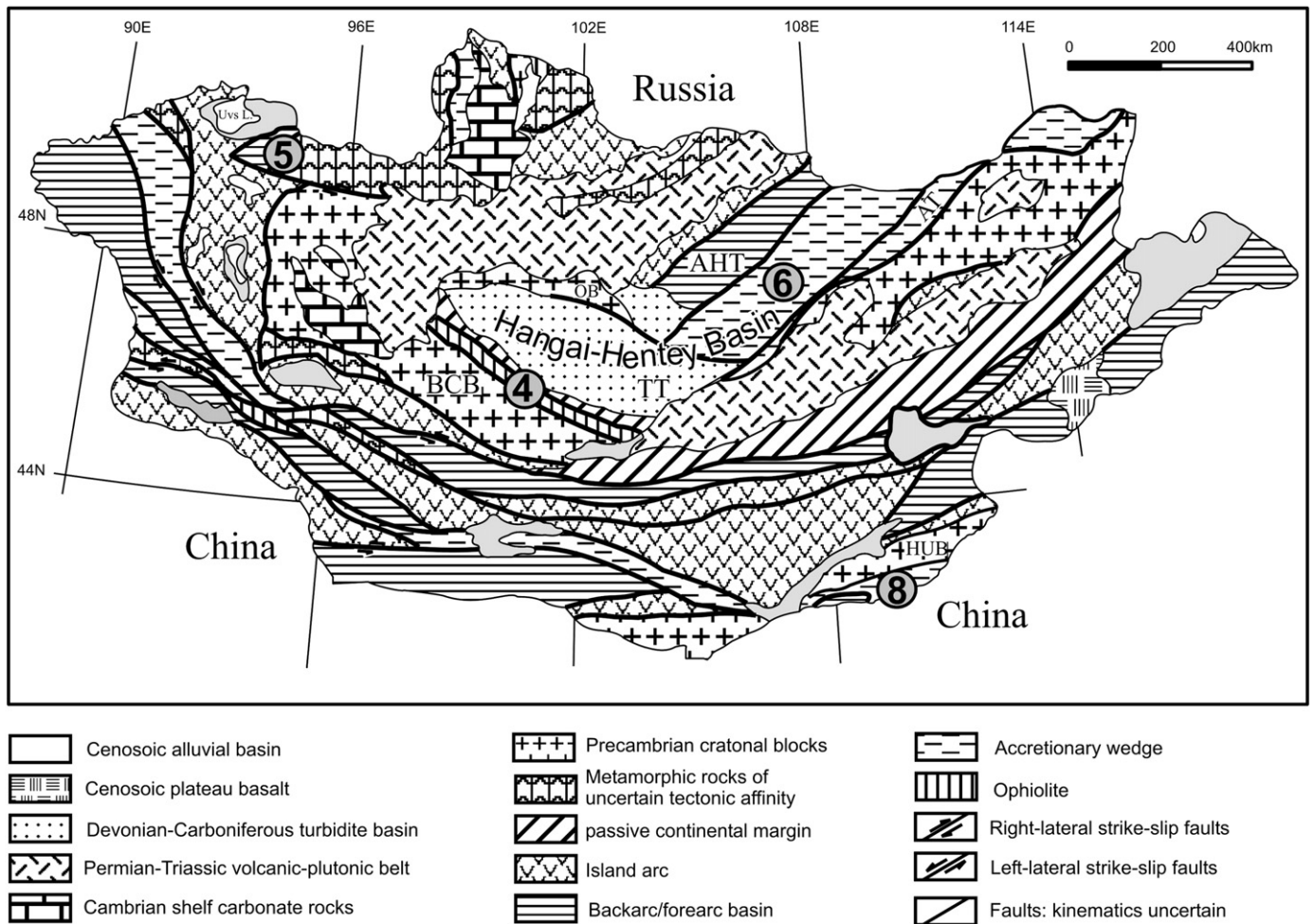


**Fig. 4.** The scheme of main terranes of Mongolia (modified after Badarch et al., 2002). Numbers in circles are OIB-hosting accretionary complexes and terranes: 4 – Bayanhangor, 5 – Agardag, 6 – Ulaanbaatar, 8 – Solonker. Abbreviations: BCB – Baydrag Cratonic Block; HUB – Hutag Uus Block; JB – Orhon Block; AT – Adatsag Terrane; AHT – Aspalt-Hairhan Terrane; TT – Tetslerleg Terrane. The age of passive margin, island-back-fore arc, accretionary and ophiolitic terranes vary from the Late Neoproterozoic to the Late Paleozoic.

sheets and blocks in mélangé where they are associated with OPS sediments containing microfossils: massive limestone, siliceous slope facies and pelagic chert (Table 1). The Char oceanic units were possibly displaced hundreds or even thousands of kilometers away from the place of their initial accretion due to the subsequent strike-slip faulting caused by the clockwise rotation of the Siberian continent (Buslov et al., 2001).

The plume magmatism in the northwestern part of the Paleo-Asian Ocean formed oceanic islands later incorporated into the Solonker AC (no. 8, Fig. 1), the formation of which marked the closure of the ocean in Permian time (Xiao et al., 2003; Windley et al., 2007). The Solonker suture or AC of the Inner Mongolia–Daxinganling orogenic belt, including the Hegenshan ophiolite (Miao et al., 2008), is located south of the Hutag Uul Block at the Mongolia–China border and consists of fragments of ophiolite, mélangé, clastics and limestone (Fig. 4). The mélangé contains blocks of tholeiitic pillow basalt, tuff, and Permian radiolarian chert and massive limestone (Badarch et al., 2002; Table 1). All these units are typical of an oceanic island setting.

### 2.3.2. Paleo-Pacific Ocean (Late Paleozoic–Mesozoic)

In the Paleo-Pacific Ocean, paleoislands and plateaus formed from the Carboniferous until the Late Jurassic and later were incorporated into ACs of the 6000 km long Circum-Pacific accretionary megabelt (Fig. 1; Dobretsov et al., 1994; Maruyama et al., 1997). The ACs of Japan comprise Akioshi–Sawadani seamounts (Carboniferous), Maizuru

plateau, Akasaka–Kuzuu seamounts (Permian), and Late Jurassic Mikabu (Sorachi) plateau (Figs. 1 and 5a–c; Maruyama et al., 1997).

The Carboniferous Akioshi–Sawadani seamount chain was formed over the Farallon Plate in the western Paleo-Pacific Ocean and accreted to the Yangtze Block during the Permian oceanic subduction (Fig. 5a; Maruyama et al., 1997). The fragments of these seamounts are presently hosted by the Akiyoshi AC (no. 9, Fig. 1, 6b), which includes OIB-type basalts and limestone-dominated OPS sediments of Middle Carboniferous–Permian age (Table 1; Sano and Kanmera, 1991). The Khabarovsk AC (Fig. 6a) comprises two OPS units of different ages based on paleontological data: Carboniferous–Permian and Triassic–Early Jurassic (Table 1). Each unit consists of pelagic chert, shallow-water limestone and basalt (Shevelev, 1987; Bragin, 1992; Suzuki et al., 2005). We suggest that the older unit can be correlated with the Akiyoshi AC because of the close ages of limestone and chert, similar lithologies and similar geochemistry of associated basalts (Table 3; Figs. 9–12). The younger OPS unit can be correlated with the Mino–Tamba AC, because it consists of Triassic ribbon chert and reef limestone overlapped by Jurassic siliceous mudstone (Suzuki et al., 2005).

In Permian time the Akasaka–Kuzuu seamount chain was formed over the Izanagi plate and later accreted to the Yangtze continental margin (Table 1; Fig. 5b) to form the Mino–Tamba AC (no. 11 in Fig. 1; Maruyama et al., 1997). The Mino–Tamba belt occupies a large part of central and Southwest Japan (Fig. 6b) and is thought to extend north to the Sikhote-Alin and northeast to China (Kojima et al., 2000).



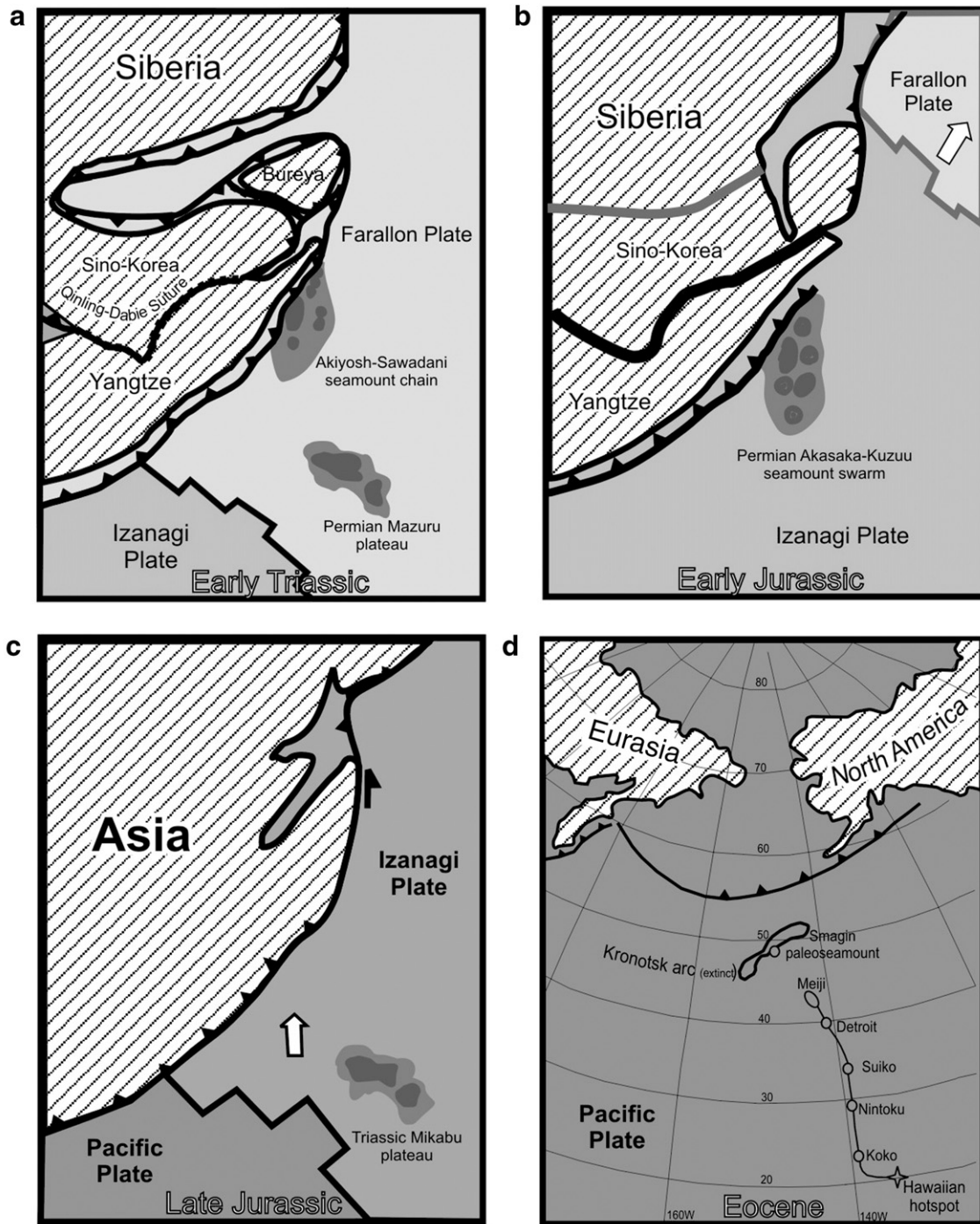


Fig. 5. Paleogeographic reconstructions for the East Asia active margin. Modified from Maruyama et al., 1997 (a–c) and Shapiro et al., 2007 (d).

Ishiwatari and Nakae (2001) showed that there are both Carboniferous and Permian basalt units in the Tamba part of the AC, whereas Sano and Kojima (2000) and Kojima et al. (2000) correlate only the Permian basalt unit. The Mino-Tamba OPS units are similar to those of the Samarka terrane in the southern Sikhote-Alin of the Russian Far East (no. 11, Figs. 1 and 6a) and are considered to be a single tectonostratigraphic unit formed along the continental margin of East Asia (Kojima et al., 2000). The Mino-Tamba AC comprises Permian carbonates and Lower Permian to Upper Jurassic bedded radiolarian cherts with related siliceous rocks overlying the OIB-type basaltic succession (Table 1; Sano and Kojima, 2000; Kojima et al., 2000; Nakae, 2000; Ishiwatari and Nakae, 2001).

During the Triassic the Mikabu plateau was formed. As a result of the Late Jurassic–Early Cretaceous oblique subduction of the Izanagi plate (Fig. 5c) the plateau was accreted to the East Asian active margin and incorporated into the Chichibu AC (no. 13, Figs. 1, 6b; Maruyama et al., 1997). The Chichibu belt is located south of the Mino-Tamba AC and consists of three terranes: northern Chichibu, Kurosegawa and Southern Chichibu (Fig. 6b). The Southern Chichibu AC (Sambosan) hosts voluminous OIB-type basalts associated with Triassic–Jurassic chert-dominated OPS (Table 1). Based on the suggested Triassic age of basalts (Onoue et al., 2004) and the reconstructions made by Maruyama et al. (1997) the OIBs hosted by the Chichibu AC may have been derived from the Mikabu plateau. A Russian analogue of the

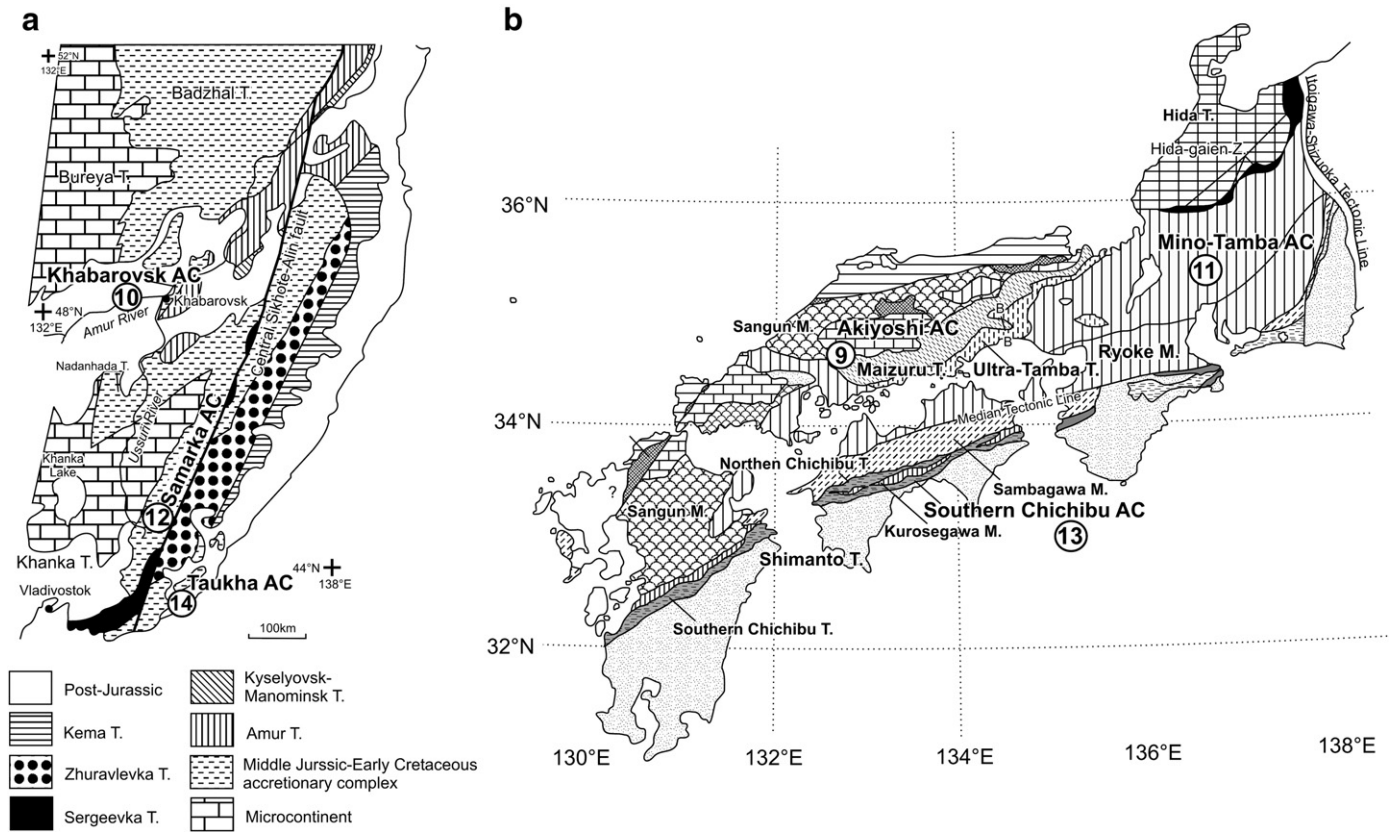


Fig. 6. Tectonic framework of Russian Far East (a) and Southwest Japan (b). Modified from Kojima et al., 2000. Abbreviations: AC – accretionary complex, T – terrane, M – metamorphic belt, Z – tectonic zone. Numbers in circles are accretionary complexes: 9 – Akiyoshi, 10 – Khabarovsk, 11 – Mino–Tamba, 12 – Samarka, 13 – Southern Chichibu, 14 – Taukha.

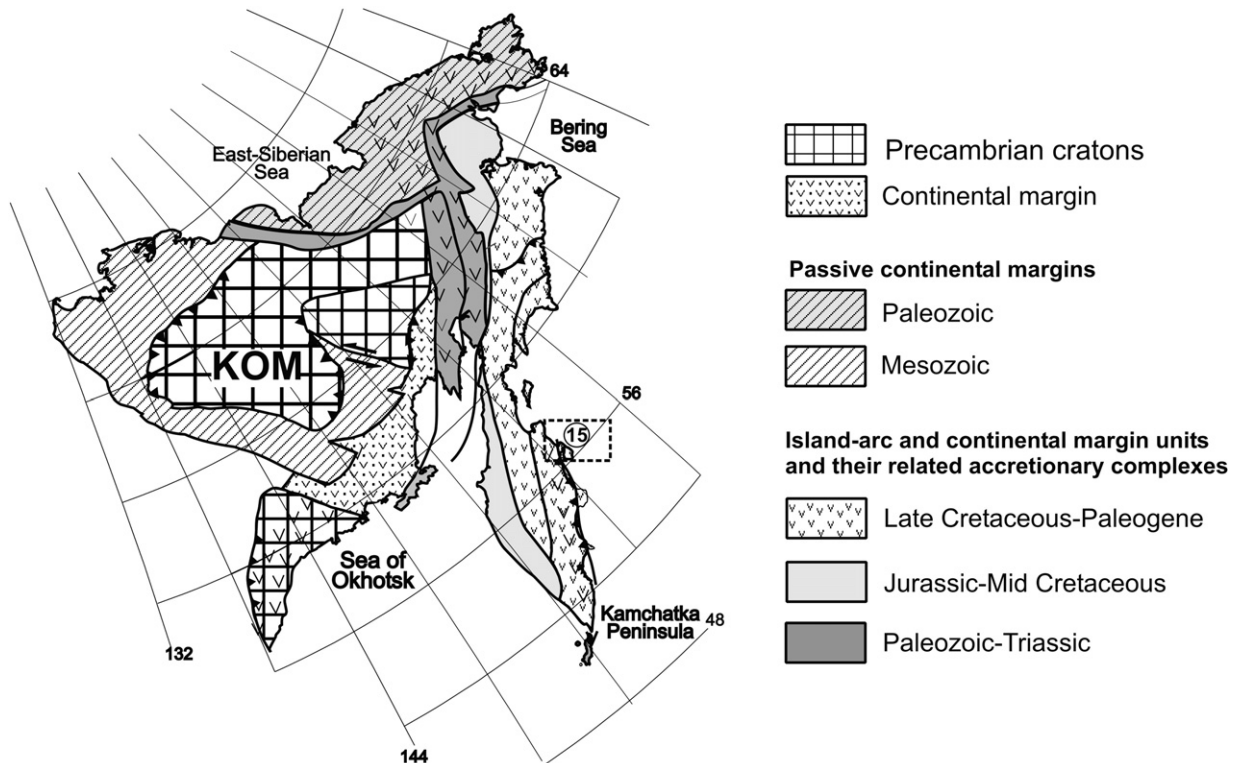


Fig. 7. Main tectonic units of Northeast Asia (northeastern Russia). The location of the Kamchatka Cape AC hosting the Smagin paleoseamount (number 15 in circle) is outlined by the dashed quadrangle. KOM – Kolyma–Omolon microcontinent at the NE of the Siberian Platform. Modified from Parfenov et al. (2006).



**Table 2**  
Original and borrowed geochemical data used in the review: references and analytical methods.<sup>a</sup>

AC's (grouped by geography)	Samples	Type of available data: published (references) or original	Analytical methods		No. of AC in figures
			REE	HFSE, LILE and others	
<i>Russian Altai, Kazakhstan</i>					
Kurai	1) KR82-KR400 <sup>b</sup> 2) 144–165, 96-56-1, C-80a-04	1) Utsunomiya et al., 2009; 2) Safonova et al., 2008	1) ICP MS 2) INAA, ICP MS	1) ICP MS 2) INAA, SR XRF, ICP MS	1
Katun	1) U45–U52; 2) E4068–E4133	1) Utsunomiya et al., 2009; 2) Original	1) ICP MS 2) INAA	1) ICP MS 2) INAA, SR XRF	2
Zasur'ya	1) 96–71, 96–83; 2) E2921, B2921, V2921, 97-120-5 3) Zas-nn-08	1) Safonova et al., 2004; 2) ME: Safonova et al., 2004; TE – original <sup>c</sup> 3) Original	1) INAA 2) INAA 3) ICP MS	1) SR XRF 2) SR XRF 3) ICP MS	3
Char	1) 95–83 2) 97-101–97-119-3	1) Safonova et al., 2004; 2) ME: Safonova et al., 2004; TE – original	1) INAA 2) INAA	1) SR XRF 2) SR XRF	7
<i>Mongolia–China</i>					
Bayanhongor	1) BHR-1–BHR-8 2) BHK-1–BHK-3	1) Ryazantsev, 1994; 2) Kopteva et al., 1984	No information		4
Agardag	T97A23–T97T44	Pfander et al., 2002	ICP MS	XRF, ICP MS	5
Ulaanbaatar	TG2–TG4	Original	ICP MS	ICP MS	6
Solonker	21DW34–21DW43	Miao et al., 2008	ICP MS	ICP MS	8
<i>Russian Far East</i>					
Khabarovsk	Am-07-07	Original			10
Samarka	L46–L237	Simanenko et al., 2009	ICP MS	ICP MS	12
Taukha	1) TH-1–TH-20 2) F05	1) Khanchuk et al., 1989a; 2) Original			14
Kamchatka	D722–D723	Original	ICP MS	ICP MS	15
<i>Central and southwest Japan</i>					
Akiyoshi	TSK1-2–TSK3-5, 50706–61110 <sup>b</sup>	Sano et al., 2000	INAA	INAA, XRF	9
Mino-Tamba	1) M-nn-07 2) 51505–83102 3) 0522–40522 <sup>b</sup>	1) Original; 2) Sano et al., 2000 3) Ichiyama et al., 2008	1) ICP MS 2) INAA 3) INAA	1) ICP MS 2) INAA, XRF 3) INAA, XRF	11
S. Chichibu	90906–13002 <sup>b</sup>	Tatsumi et al., 2000	No data	XRF	13

<sup>a</sup> Major element concentrations are available for all the localities and have been determined by the XRF method.

<sup>b</sup> For the purpose of space saving the samples numbers were shortened to four or five last characters compared to those cited in the original paper.

<sup>c</sup> Abbreviations: ME – major elements, TE – trace elements, LILE – large-ion lithophile elements.

Southern Chichibu is the Taukha AC (no. 13 in Fig. 1; Golozubov et al., 1992; Kojima et al., 2000) located at the southern end of the Sikhotealin' Mts. (Fig. 6a). Similarly, the Taukha terrane consists of radiolarian chert, siliceous mudstone, sandstone, synsedimentary folded clastic rocks, and intraplate basalts or paleoguyots (Khanchuk et al., 1989a; Golozubov et al., 1992; Safonova, 2009). The “carbonate cap” limestones are directly underlain by OIB-type basalts and contain Middle–Late Triassic fauna (Table 1), while the cherts contain radiolarians of Middle Triassic–Late Jurassic and Jurassic–Early Cretaceous ages (e.g. Khanchuk et al., 1989a; Golozubov et al., 1992).

Around 15 Ma Japan split off East Asia (Maruyama et al., 1997; Khanchuk and Kemkin, 2003) resulting in the separation of once unified OPS units including fragments of oceanic islands and accretionary complexes, which presently outcrop on both shores of the Sea of Japan: Russian Far East and Southwest Japan. Most accretionary prisms have been built along the Pacific margin of these islands, like in other Pacific-type orogenic areas (Santosh et al., 2009b), and those in Southwest Japan have been less destroyed by later processes of metamorphism and tectonics.

In the Late Cretaceous, the hot spot magmatism continued over the Pacific Plate and resulted in the formation of the Smagin paleoseamount, which probably represents an oldest seamount of the Emperor Chain (Saveliev, 2003; Portnyagin et al., 2005). The OIB-type basalts are associated with Albian–Cenomanian cherts (Table 1). The subduction of the Pacific plate resulted in the accretion of the paleoseamount to the Kronotsky island arc (Santonian–Campanian, ca 85–70 Ma; Fig. 5d). Later, they were amalgamated with the NE margin of Asia and incorporated into the Kamchatsky Cape AC of Eastern Kamchatka at about 10 Ma (no. 15, Fig. 7; Khotin and Shapiro, 2006; Shapiro et al., 2007).

More detailed sedimentological descriptions of the above mentioned OPS units with OIB-type basalts and detailed mechanisms of their accretion to island arcs and continental margins are available in the publications mentioned in Table 1. Schematic stratigraphic columnar sections for each plume-related basaltic unit have been constructed for Altai, Russian Far East and Japan ACs (Safonova, 2009). For those of Mongolia and Kamchatka see Badarch et al. (2002) and Khotin, Shapiro (2006), respectively. Generally, most Pacific-type orogenic belts formed during collision of Gondwana-derived blocks (Buslov et al., 2001; Santosh et al., 2009b) are characterized by similar mechanisms of accretion. Tectonic cartoons illustrating scenarios of accretion are shown in Buslov et al. (1993) and Dobretsov et al. (1995) for Altai–Sayan; Xiao et al. (2003) and Windley et al. (2007) for Mongolia; Khanchuk, Kemkin (2003) and Kemkin (2006) for Russian Far East; Isozaki et al. (1990), Isozaki (1997), Kimura et al. (1994), Maruyama et al. (1997), Koizumi, Ishiwatari (2006) for Japan, and Shapiro et al. (2007) for Kamchatka.

### 3. Analytical methods and sample selection

This paper presents both original and published geochemical data. The original data were obtained for the accretionary complexes of Russian Altai (Kurai<sup>1</sup>, Katun<sup>1</sup>, Zasur'ya ACs<sup>1</sup>), East Kazakhstan (Char AC<sup>1</sup>), Mongolia (Ulaanbaatar), Far East (Khabarovsk, Samarka, Taukha), Japan (Mino-Tamba<sup>1</sup>) and Kamchatka (Smagin<sup>1</sup>) from the least deformed outcrops of pillow lavas and flows (Tables 2–4; Table 4

<sup>1</sup> A part of the analyses included in the present review was published before. For details see Table 2.

in the Appendix is an electronic supplementary item, which is available online XXX). The samples were ground in an agate mill. Abundances of major elements were determined at the Institute of Geology and Mineralogy SB RAS by X-ray fluorescence spectrometry (XRF) using a “Nauchpribor” device. The analytical procedure followed the Russian state analytical standard OST-41-08-212-82 Mingeo SSSR; relative standard deviations (RSD) are within 5%, and totals were within  $100 \pm 1\%$ . Trace elements were analyzed by inductively coupled plasma mass-spectrometry (ICP MS) in the Tokyo Institute of Technology (ThermoElemental VG 244 PlasmaQuad 2 LA ICP MS; on fused glass beads) and in the Institute of Geology and Mineralogy SB RAS (ICP MS (Finnigan Element; on powdered samples)) using the protocols of Jenner et al. (1990). BHVO-1, BCR-1 and JB-3 were used as international reference materials to estimate precision and accuracy. The analytical errors are estimated as 2–7% for rare earth elements (REE) and high-field strength elements (HFSE). The Samarka and Taukha basalts were analyzed at the Far East Geological Institute FEB RAS: major elements were determined by a standard “wet chemistry” technique and trace elements by ICP MS (VG Plasmaquad 2). For details of that ICP MS analytical procedure see Rasskazov et al. (2004).

The original data were selected from a larger population. The subset was screened for least alteration on the criteria of preservation of igneous textures, petrographic freshness, low losses on ignition – L.O.I. (Tables 3 and 4), coherent chondrite normalized REE patterns and primitive mantle-normalized multi-element (trace element) spectra for given igneous suites (Figs. 11, 12).

The published analytical data on the Kurai, Katun, Zasur'ya and Char ACs were obtained by XRF (major elements), synchrotron radiation XRF (Ni, V, Rb, Sr, Y, Zr, Nb), instrumental neutron activation analysis – INAA (REE, Hf, Ta, Th, U, Rb, Ba, Cr) and ICP MS (REE, Ni, Rb, Sr, Y, Zr, Nb, Ba, Ta, Th, Hf, U; Safonova, 2005; Safonova et al., 2004, 2008). The synchrotron radiation XRF technique is described in Phedorin et al. (2000). The INAA was performed by using Ge detectors for  $\gamma$ -rays higher than 30 keV and below 2000 keV. All the data are of good quality and well within international standards; the analytical errors on most REE and HFSE were within 5–10% (Safonova, 2005). The data on the Akiyoshi, Mino-Tamba and Chichibu ACs of Japan (Tables 3, 4) were obtained by XRF (major elements plus V, Cr, Ni, Rb, Sr, Y, Zr, Nb, Ba) and INAA (REE, Hf, Ta, Th, Cr, Ba). The error ranges of INAA are 3–6% for Cr, La, Ce, Sm and Eu, and 10–20% for Hf, Ta, Th, Ba, Yb and Lu (Ichiyama et al., 2008). Description of analytical procedures is given in relevant papers (Sano et al., 2000; Koizumi and Ishiwatari, 2006; Ichiyama et al., 2008; Tatsumi et al., 2000), however these papers presented no information on the XRF analytical errors.

#### 4. Geochemical features of intraplate basalts

The paper presents a compilation of published and original major and trace-element data (Tables 2–4 and the references therein). Unfortunately, the full trace-element data on the Bayanhongor, Khabarovsk, Taukha and Chichibu ACs are very limited. For convenience, in the succeeding diagrams, we have divided the dataset into two groups based on their geographical location and relation to the Paleo-Asian and Paleo-Pacific Oceans, respectively: 1) those recovered from accretionary complexes of Altai–Sayan (Kurai, Katun, Zasur'ya), Mongolia (Bayanhongor, Agardag, Ulaanbaatar, Solonker) and East Kazakhstan (Char; Fig. 8a, plots a–d in Figs. 9–12, 13a,c), and 2) those from accretionary complexes of Japan (Akiyoshi, Mino-Tamba, Southern Chichibu), Russian Far East (Khabarovsk, Samarka, Taukha) and Kamchatka (Smagin; Fig. 8b, plots e–h in Figs. 9–12, 13c,d).

Before presenting geochemical data on the intraplate basalts of the Paleo-Asian and Paleo-Pacific Oceans, we briefly address the petrographic features of intra-late basalts and the effect of post-magmatic alteration and its related element mobility on the chemical composition.

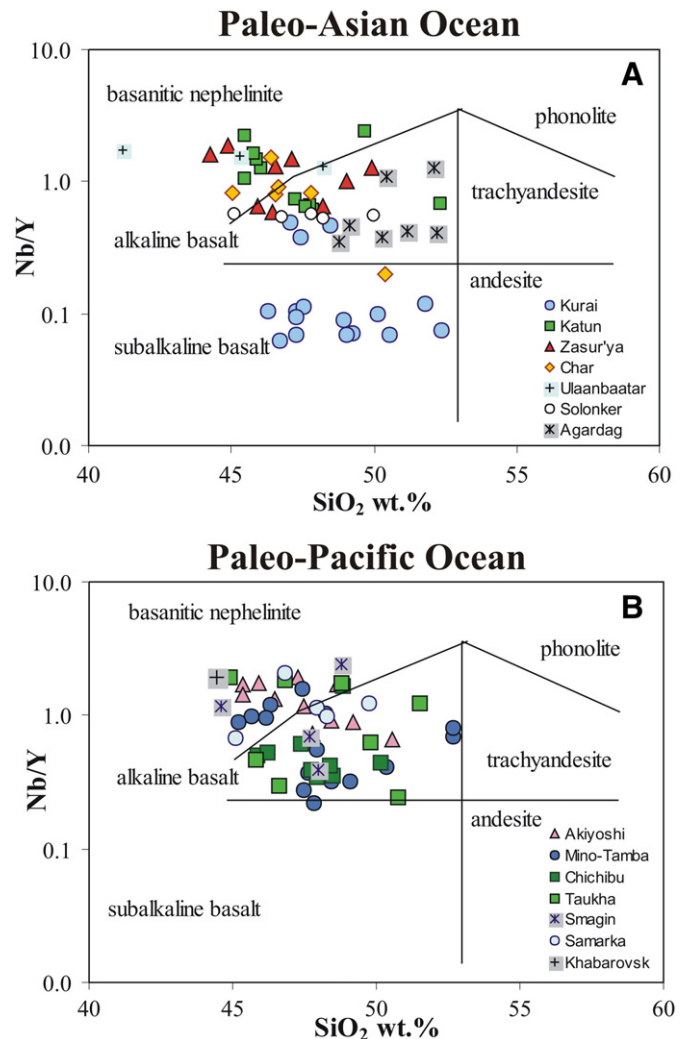


Fig. 8. Nb/Y versus  $\text{SiO}_2$  classification diagram (Winchester and Floyd, 1977).

#### 4.1. Petrography

Most original samples of basalts display similar petrographic textures, ranging from fine- to medium-grained porphyritic to aphyric, with porphyric lavas dominant. Amygdaloidal textures are also typical with amygdales usually filled by calcite and chlorite. The phenocrysts in the porphyritic varieties are plagioclase, clinopyroxene and olivine. Groundmass is variolitic, microlitic or hyalopilitic. Opaque minerals, principally magnetite, are present as accessory phases. In general, the Late Neoproterozoic and Early Paleozoic basalts have undergone stronger post-magmatic alteration than the Late Paleozoic and Mesozoic basalts. Olivine, pyroxene and volcanic glass are partly or completely replaced by chlorite and epidote, and plagioclase by albite. Although basalts have been metamorphosed in the greenschist facies and contain abundant alteration minerals such as epidote, chlorite and albite, they display well-preserved igneous textures. For more detailed petrographic data see the referred publications (Table 2).

#### 4.2. Secondary alteration and element mobility

As far as most oceanic basalts found in Paleozoic–Mesozoic accretionary complexes have undergone sub-marine hydrothermal alteration, poly-phase deformation and greenschist to epidote–amphibolite facies metamorphism, some elements may have been

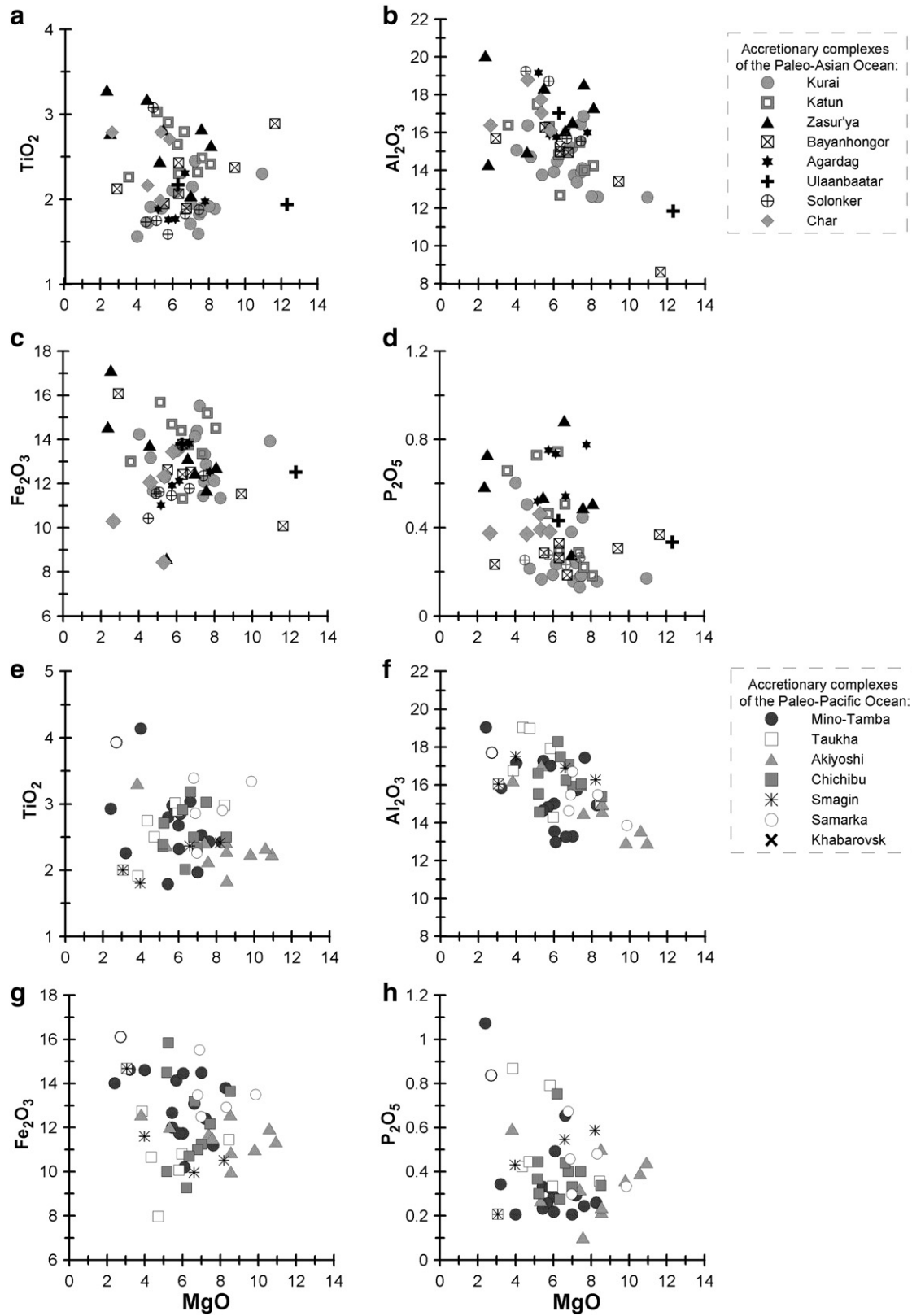


Fig. 9. MgO versus major element data for OIB-type basalts from the accretionary complexes of Russia, Mongolia and Japan.

mobile. The mobility of Rb, K, Na, Sr, Ba, Fe, and Pb in Precambrian and Phanerozoic pillow basalts is well documented (e.g. Polat et al., 2007 and the references therein), and our previous studies confirmed the mobility of these elements in the Altai–Sayan basalts (see Safonova, 2005; Safonova et al., 2008). There is general agreement that REE,

HFSE, and some transition metals (V, Ni, Cr) are least sensitive to mobility (e.g. Winchester and Floyd, 1977; Ludden and Thompson, 1978). MgO enrichment due to chloritization can be suggested for old OIB-type basalts (e.g. Komiya et al., 2004), but in that case there must be correlation between MgO and L.O.I. or C.I.A. (chemical index



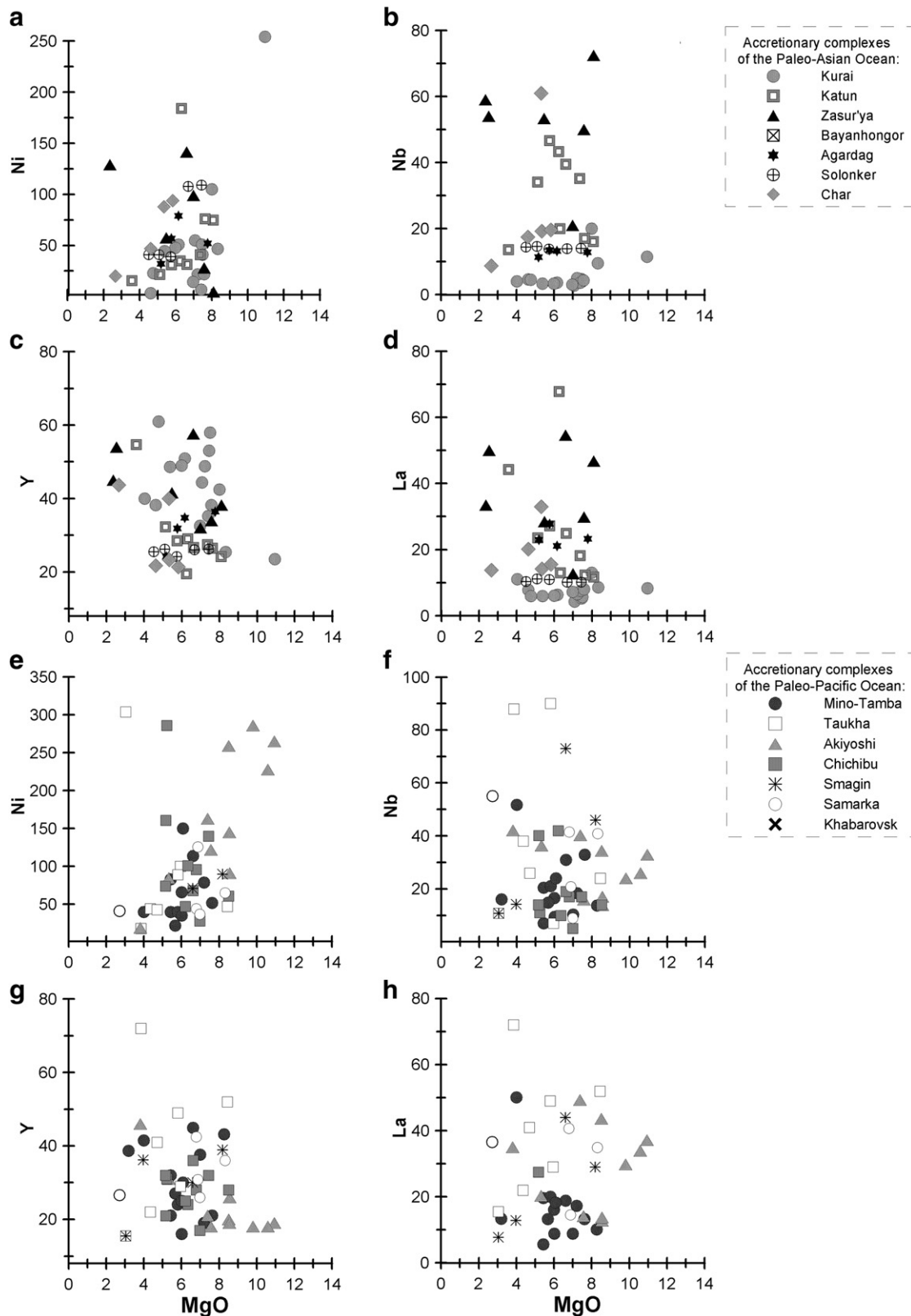
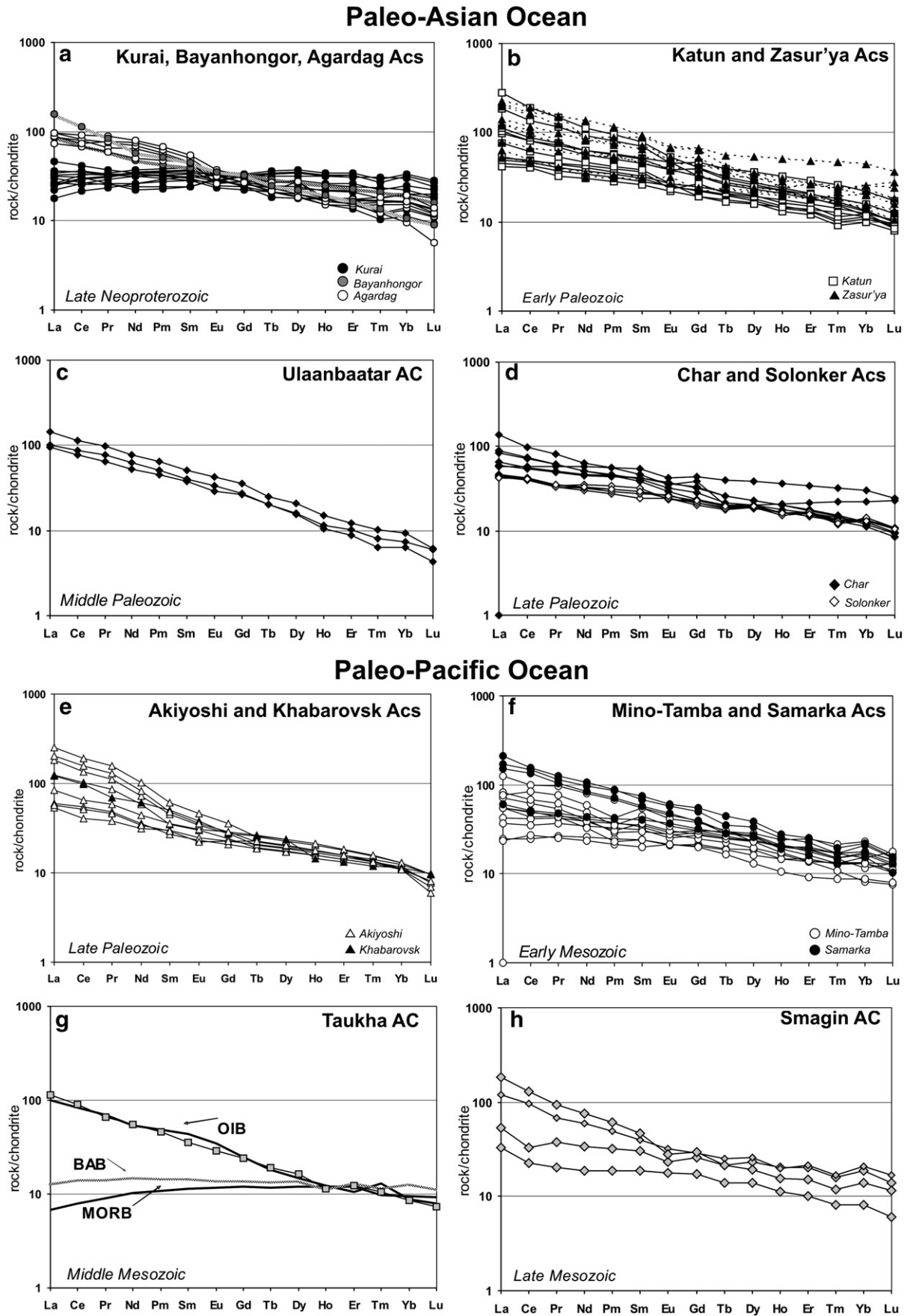


Fig. 10. MgO versus trace-element data for OIB-type basalts from the accretionary complexes of Russia, Mongolia and Japan.

of alteration; Nesbitt, Young, 1982). However, the plots of MgO versus L.O.I., C.I.A., Sr, Ba and other mobile elements (not shown here) revealed no trends. Therefore, we assumed that MgO was relatively immobile during secondary alteration and used diagrams where MgO versus other major and trace elements (Sections 4.3, 4.4). Light REE

(LREE) are more sensitive to secondary processes compared to middle REE and heavy REE (HREE), however the mobility of REE takes place only at high water/rock ratio or during carbonatization (Humphris, 1984), which is not observed in our case. Besides, evidence for low mobility of HFSE, REE (except Eu) and, to a lesser degree, Th includes



**Fig. 11.** Chondrite-normalized rare-earth element patterns. OIB, MORB and normalization values are from Sun and McDonough (1989). BAB are from Dampare et al. (2008), Many and Maboko (2008) and GEOROC database ([www.georoc.mpch-mainz.gwdg.de/georoc](http://www.georoc.mpch-mainz.gwdg.de/georoc)). The horizontal axis shows symbols of all elements, including those without analyses, because of different sets of trace elements available for different samples. For details see Tables 3 and 4.

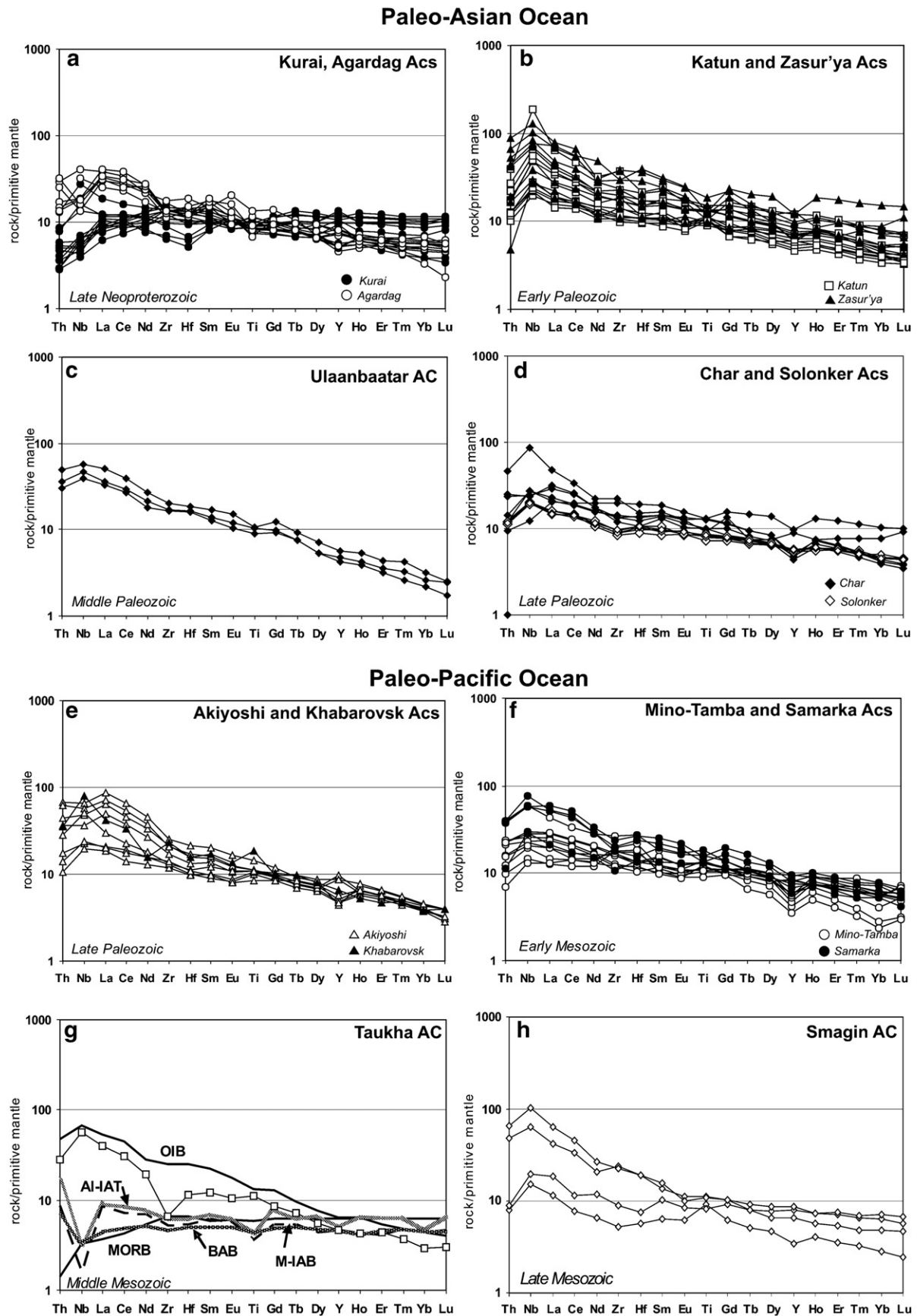


**Fig. 12.** Primitive mantle-normalized multi-component trace-element diagrams. OIB, MORB and normalization values are from Sun and McDonough (1989). The averaged data on the Aleutian (AI-IAB), Mariana (M-IAB) island-arc basalts and back-arc basalts (BAB) are from GEOROC database ([www.georoc.mpch-mainz.gwdg.de/georoc](http://www.georoc.mpch-mainz.gwdg.de/georoc)) and from Dampare et al. (2008) and Many and Maboko (2008) for BAB. The horizontal axis shows symbols of all elements, including those without analyses, because of different sets of trace elements available for different samples. For details see Tables 3 and 4.



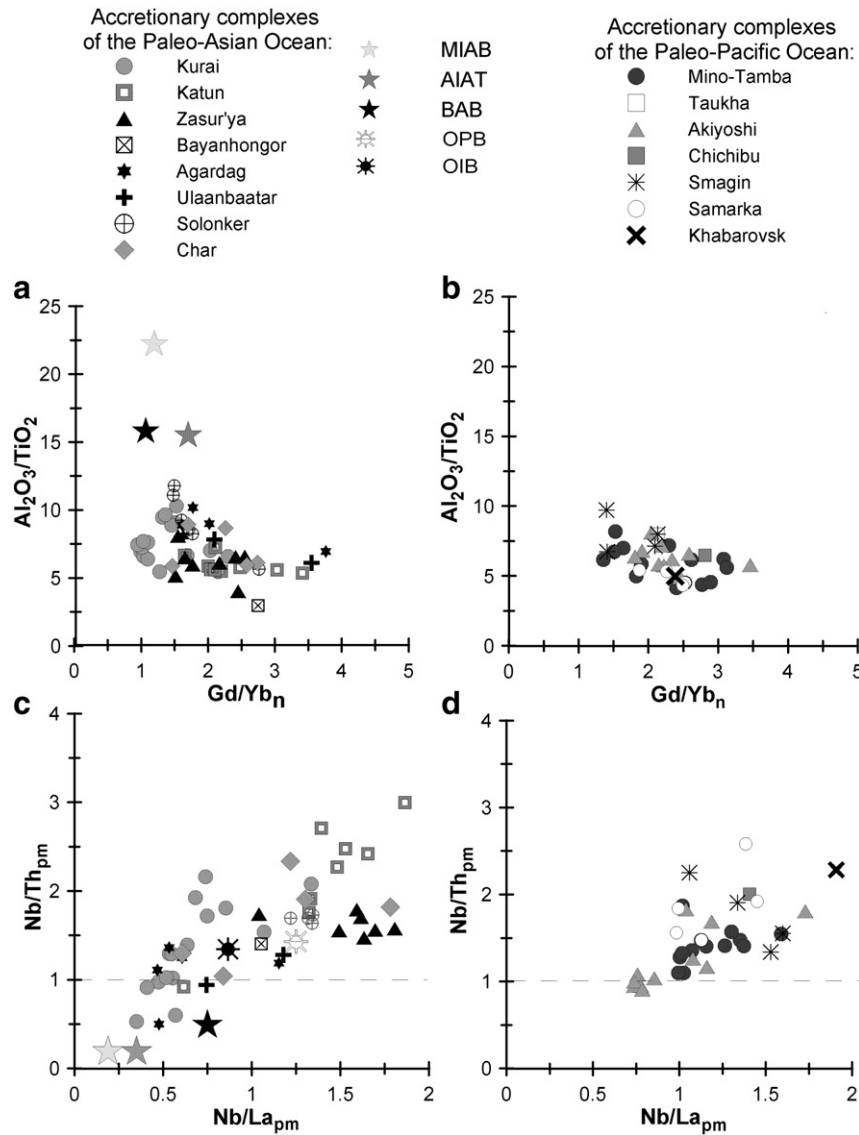


**Fig. 13.**  $Al_2O_3/TiO_2$  versus  $Gd/Yb_n$  (a, b) and  $Nb/Th_{pm}$  versus  $Nb/La_{pm}$  (c, d) indicating low to medium degree of melting (a, b) and absence of crustal contamination (c, d) compared to other OIBs, oceanic plateau basalts (OPB), back-arc (BAB) and island-arc basalts (IAB). The data on the Aleutian (AI-IAB) and Mariana (M-IAB) and BAB are from GEOROC database ([www.georoc.mpch-mainz.gwdg.de/georoc](http://www.georoc.mpch-mainz.gwdg.de/georoc)) and also from Dampare et al. (2008) and Many and Maboko (2008) for BAB. OIB and MORB – from Sun and McDonough (1989).

the following: 1) there is no significant enrichment or depletion of groups of elements (e.g. light REE) in a given rock type over a range of L.O.I. (L.O.I. in the selected samples generally ranges from 1 to 5; Tables 3, 4); 2) rare-earth and trace-element diagrams of given suites of basalts associated in the field exhibit coherent patterns for Th, HFSE, and REE (Figs. 11 and 12); 3)  $Th/La_{pm}$  and  $Nb/La_{pm}$  do not correlate with C.I.A.,  $Eu/Eu^*$ , or L.O.I. (not shown here; Safonova, 2005; Safonova et al., 2008); 4)  $Zr/Hf$ ,  $Nb/Ta$ , and  $Y/Yb$  ratios for most samples are close to the primitive mantle values of 36, 18, and 10, respectively (Table 3). Rare deviations of these ratios in some samples we explain by different applied methods because the analytical error of XRF on, for example, Nb may reach 20%. For this reason, emphasis is placed on HFSE and REE.

### 4.3. Major element compositions

Analyses of 127 representative samples (73 – PAO, 55 – PPO) selected from different publications plus original data (Tables 3, 4) are illustrated in Figs. 8–12. Samples were recalculated to 100% anhydrous for inter-comparisons. The samples are dominated by

alkaline varieties according to the  $SiO_2$  versus  $Nb/Y$  classification diagram (Fig. 8; Winchester and Floyd, 1977). The subalkaline basalts are more typical of the Kurai AC. The principal major element characteristics of both groups are variable  $MgO$  contents (2–13 wt.%; the majority between 4 and 8 wt.%) and  $Fe_2O_3(tot)$  (4–10 wt.%), resulting in  $Mg\#$  between 20 and 70 (Table 3). In the  $TiO_2$ ,  $Al_2O_3$ ,  $Fe_2O_3$  and  $P_2O_5$  versus  $MgO$  diagrams (Fig. 9) the data are scattered revealing no general elevation in these elements. On average, the younger samples of the Paleo-Pacific Ocean (Fig. 9e–h) have higher  $TiO_2$  and  $P_2O_5$  contents and lower  $MnO$  than the older basalts of the Paleo-Asian Ocean (Fig. 9a–d). The  $TiO_2$  concentrations vary between 1.5 and 4.1 wt.%, and  $P_2O_5$  is in the range 0.13–1.0 wt.%, with  $P_2O_5$  showing enrichment with decreasing  $MgO$  in all groups except for the Mino-Tamba AC (Fig. 9b, d, f, h). Both  $TiO_2$  and  $Fe_2O_3(tot)$  increase slightly with decreasing  $MgO$ , suggesting that magnetite or titanomagnetite were not major fractionating phases.  $SiO_2$  spans 45–55 wt.% (average = 48 wt.%);  $Al_2O_3$  varies between 13 and 20 wt.% and generally increases with decreasing  $MgO$  suggesting simultaneous fractionation of clinopyroxene and plagioclase (Fig. 9b, f).

#### 4.4. Trace-element compositions

The concentrations of trace elements (Tables 3 and 4) are illustrated in Figs. 10–12. The concentrations of Ni and Cr are typically low, with averages around 80 and 160 ppm, respectively. These are consistent with the evolved nature of these samples indicated by the generally low Mg#. No samples display both high Ni and Cr, which is thought to be consistent with a primitive magma composition (Fig. 10a, e; Tables 3, 4).

The positive correlation between MgO and Ni is presumably controlled by olivine and pyroxene fractionation. More specifically, decreasing Ni with decreasing MgO indicates early fractionation of olivine (Fig. 10a, e). The concentrations of Nb (3–130 ppm), Y (16–70 ppm) and Zr (60–480 ppm) in the Katun, Zasukh, Char and Akiyoshi basalts show weak to moderate increase with decreasing MgO as expected by fractionation of plagioclase, olivine and clinopyroxene (Fig. 10a–c, e–g). The majority of the samples (80%) have Zr/Nb ratios from 1.8 to 14, similar to those found in many OIBs, e.g., the Emperor–Hawaii seamount chain (Regelous et al., 2003), although the samples from the Kurai AC have significantly higher Zr/Nb ratios of about 31 (av.), similar to oceanic plateau basalts, e.g., Ontong Java Plateau (Mahoney et al., 1993). Ti/Zr ratios range from 75 to 266 (Tables 3, 4) implying different conditions of formation, controlled by either the composition of the source, the nature of partial melting and/or the extent of titanomagnetite fractionation.

All groups of basaltic lavas (except for the Kurai AC) have clearly LREE-enriched rare-earth patterns:  $La_N = 23.29–282.5$ ,  $La/Yb_N = 1.74–16.21$ ,  $La/Sm_N = 1.02–3.62$ ,  $Gd/Yb_N = 1.35–7.47$  (Fig. 11b–h).  $Eu/Eu^*$  ranges from 0.72 to 1.39 with an average value of 1.07<sup>2</sup>. The patterns of most samples possess zero to small Eu anomalies ( $Eu/Eu^* = 0.91–1.11$ ) with the exception of the Kurai basalts possessing both negative and positive Eu anomalies ( $Eu/Eu^* = 0.78–1.23$ ) possibly due to the secondary alteration (see Section 4.2). The Kurai basalts, which have been interpreted as oceanic-island or oceanic plateau basalts, have nearly flat REE patterns (Fig. 11a) with less fractionated LREE:  $La_N = 17.67–54.17$ ,  $La/Yb_N = 0.71–4.85$ ,  $La/Sm_N = 0.62–1.59$ ,  $Gd/Yb_N = 0.94–2.30$ . The REE patterns of the Kurai OPB-type lavas are similar to those of the Nauru Basin and Ontong–Java plateau basalts (Safonova et al., 2004, 2008; Utsunomiya et al., 2009), whereas the other patterns are close to typical OIB. HREE concentrations are slightly higher in the Kurai basalts compared to other localities, however, the degree of HREE fractionation is higher in the latter (Fig. 11; Tables 3, 4). Although previously the Agardag basalts were interpreted as BAB only, the REE patterns of a number of high-Ti samples selected from Pfander et al. (2002) are actually more similar to the typical OIB and therefore different from average BAB (Fig. 11a, g; GEOROC database; Dampare et al., 2008; Manya and Maboko, 2008).

Fig. 12 displays trace and minor element data for selected samples normalized to the primitive mantle (McDonough and Sun, 1995). The multi-component trace-element diagrams of basalts from all the accretionary complexes except for the Kurai, Agardag and Akiyoshi display prominent positive Nb anomalies with respect to La and Th ( $Nb/La_{pm} = 1.2–1.9$ ;  $Nb/Th_{pm} = 1.02–5.6$  for 85% of data; Fig. 12b–d, F–H). The Kurai, and a part of Agardag basalts, are characterized by negative anomalies of Nb and Ti, which are distinctive features of oceanic plateau basalt. For example, the Ontong Java Plateau, the world's largest oceanic igneous province, also shows low Nb and Ti abundances (Mahoney et al., 1993). Nb negative peaks in respect to La in the Kurai and Agardag samples are present in some OIB, possibly

due to endogenous contamination with recycled crust material (Saunders et al., 1988). Ti negative peaks in the multi-element spectra mentioned in some OIB-type basalts (e.g., Polat et al., 1999) may reflect fractionation of Ti-compatible deep-seated minerals such as rutile and perovskite.

The patterns for the Kurai, partly Agardag and Akiyoshi basalts weakly peak at La and have smoother convex-up patterns through La, Nb and Th ( $Nb/La_{pm} = 0.7–1.0$ ). In all samples Th is depleted in respect to Nb and La ( $Th/La_{pm} = 0.5–0.9$ ;  $Nb/Th_{pm} = 1.0–2.1$ ; Tables 3, 4; Fig. 12). Similar trace-element patterns have been documented for many Phanerozoic transitional to alkaline ocean island basalts (e.g. Chen et al., 1991; Weaver, 1991; Regelous et al., 2003). Many samples are characterized by negative Zr anomalies ( $Zr/Zr^* = 0.19–0.38$ ) suggesting their mantle source within the garnet stability field. Similarly to the REE distribution patterns, the Agardag basalts under consideration are characterized by the trace-element spectra quite different from those typical of both IAB and BAB and close to OIB (Fig. 12a, g). Smaller abundances of Nb, Zr, Hf and Ti compared to neighboring REE (Fig. 12a) in a part of Agardag samples may resemble those in shoshonites, whose occurrences are confirmation of the previously proposed arc or back-arc settings. However, compared to the Agardag samples, typical shoshonitic basalt compositions are characterized by lower  $TiO_2$  (0.6–1 versus 2.0),  $Fe_2O_3$  (8.6 versus 11.2) and Nb (11 versus 16.1) and much higher Th and K (e.g. Joplin et al., 1972; Wang et al., 2006; Conticelli et al., 2009). Even taking into account the secondary alteration we cannot disregard these facts because alkalis usually increase in altered oceanic basalts.

In the  $Al_2O_3/TiO_2$  versus  $Gd/Yb_n$  diagram (Fig. 13a, c) the data points form a rather compact but elongated field, which is almost parallel to the x-axis. OIB-type basalts are characterized by higher  $Gd/Yb_n$  on average and notably lower  $Al_2O_3/TiO_2$  compared to MORB, island-arc and back-arc basalts (IAB and BAB, respectively). This fact is important in terms of identification of OIBs in accretionary complexes, which are sometimes erroneously regarded as IAB or BAB or ophiolites (MORB). All the OIB-type samples show clear Ti enrichment and medium to strong HREE fractionation, which is likely to be a garnet signature of mantle melting. The  $Gd/Yb_n$  ratios which vary from 3.5 to 1 suggest low to medium degrees of partial melting (Fig. 13a, c).

Based on the presented data two geochemical types of Paleo-Asian Ocean and Paleo-Pacific Ocean intraplate basalts are recognized: 1) LREE, Nb and Ti enriched and 2) transitional. In the REE and trace-element diagrams the alkaline basalts are characterized by LREE-enriched patterns and positive Nb anomalies, whereas the transitional varieties (subalkaline in Fig. 8) have flatter REE regions of the patterns and display zero to negative Nb anomalies in respect to La and, to a lesser degree, Th (Figs. 11, 12). The basaltic units hosted by Kurai and Akiyoshi ACs include both rock types, whereas the other accretionary complexes are dominated by enriched varieties though incorporating transitional varieties as well (see references in Table 2). Enriched basalts are characterized by higher  $Gd/Yb_n$ ,  $Nb/La_{pm}$  and  $TiO_2$  and show medium to strong HREE fractionation.

## 5. Discussion

In order to address problems of the origin and extent of the intraplate basaltic magmatism of the Paleo-Asian and Paleo-Pacific Oceans, we will discuss specific features of the relationship between basalts and other OPS units, key geochemical features of plume-related basalts and their possible mantle sources, and evaluate the possibility of crustal contamination. We will also explain possible reasons for misinterpretation of intraplate basalts in some accretionary complexes. Special attention will be paid to ideas for future studies. All these elements help us to better understand the history of two oceans and to reach a conclusion about their mutually related or independent evolution.

<sup>2</sup>  $Eu/Eu^*$  was calculated following the method of Taylor and McLennan (1985), i.e. referenced to Sm and Gd.

### 5.1. Geological position of plume-related OPS units

The problem in identification of intraplate basalts is partly related to their occurrence within structurally complicated fold zones, i.e. accretionary complexes in our case. These AC formed during accretion of island arcs, paleoislands and sometimes back-arc units to continental margins with the subsequent closure of paleo-oceans followed by intensive deformation and faulting. Thus formed accretionary complexes are usually adjacent to much larger island-arc complexes formed over subduction zones. Therefore, when carrying out fieldwork in such settings we might expect to also find accreted fragments of paleo-oceanic seamounts consisting of basaltic pillow lavas and flows and oceanic sedimentary rocks (OPS units). Below we present several geological and structural features, which are typical of the majority of localities.

All the localities of intraplate basaltic lavas under consideration are characterized by their association with OPS units: “carbonate cap” of shallow-marine massive or bedded reefal limestone, carbonate-epiclastic-siliceous slope facies (siliceous shale, siltstone, mudstone, sandstone, lime-rich conglomerate/breccia) and pelagic bedded/radiolarian chert (Isozaki et al., 1990). Plume-related basalts, formed in an intraoceanic setting (oceanic islands, seamounts and plateaus), occur at the base of all OPS units (Safonova, 2009). Thick bodies of basalts are capped with carbonates, but thinner lava flows (up to 10 m) may be intercalated with slope facies sediments, sometimes possessing signatures of their formation on the volcano’s slopes: synsedimentary (intraformational or asymmetric) folding, brecciation, variable thickness of beds. The pelagic ribbon cherts are often folded due to later accretion and collision-related deformation to form “wavy” textures.

The older OPS units of the PAO are hosted by the Katun, Kurai, Bayanhongor and Agardag ACs and consist of thick carbonates, carbonate breccia and, to a lesser degree, epiclastic sediments. The younger complexes of the same ocean from the Zalur’ya, Ulaanbaatar, Char and Solonker ACs are dominated by pelagic chert, siliceous shale, mudstone and sandstone (Ryazantsev, 1994; Badarch et al., 2002; Sennikov et al., 2003; Xiao et al., 2003; Dobretsov et al., 2004; Safonova, 2009). The PAO oldest Kurai paleoseamount consists of a thick limestone–dolomite unit – the Baratal Formation (Buslov et al., 2001; Uchio et al., 2004). Similarly, the Akiyoshi complex, which is the oldest unit of the PPO, is famous for a huge “carbonate cap” and thick lime conglomerates (Kanmera et al., 1990; Isozaki et al., 1990), whereas the younger Mino-Tamba, Samarka, Southern Chichibu, and Taukha ACs are dominated by cherts and siliceous shales (Khanchuk et al., 1989b; Sano and Kojima, 2000; Kojima et al., 2000; Kemkin, 2006). The OPS units of the Smagin AC, which includes the oldest seamount of the Emperor Chain, consist mainly of carbonates and epiclastic rocks as well (Saveliev, 2003). It is likely that the chert and siliceous shale sequences are less stable under deformation and therefore have been poorly preserved in older and more strongly deformed accretionary complexes or buried beneath the latter during subduction. Just the absence of thick carbonate units in the Khabarovsk AC makes its proposed correlation with the Akiyoshi AC quite questionable in spite of their close ages (regarding the lower part of the Khabarovsk AC only) and similar geochemistry of OIB-type lavas (Figs. 8–13).

Frequently, blocks and sheets of OPS units occur within tectonically deformed mélanges formed during accretion and are spatially associated with nappe-thrust structures, which are typical of accretionary complexes (Sano, Kanmera, 1991; Buslov et al., 1993, 2004b; Isozaki, 1997). Mélanges may include turbidites, ophiolites and high-pressure rocks. A careful field study of such units may help us to find blocks in mélanges with direct contacts between volcanic and sedimentary rocks and to know the age of magmatism by studying microfossils.

Thus, the OPS units including OIB-type basalts, reefal limestone, bedded/radiolarian chert and epiclastic slope facies suggest their

formation in an oceanic island setting in an open oceanic realm in relation to hot spot magmatism (Safonova, 2009).

### 5.2. Crustal contamination

In the Nb/La<sub>pm</sub> versus Nb/Th<sub>pm</sub> diagram (Fig. 13c, d) most samples plot above the line of Nb/Th<sub>pm</sub> = 1, which conventionally separates crustally contaminated and non-contaminated basalts (Polat et al., 1999). Negative Nb anomalies in some basalts from the Kurai, Agardag and Akiyoshi ACs could possibly reflect some crustal contamination, however, numerous lines of geological evidence, provided by many geologists previously worked in the Kurai and Akiyoshi regions, are consistent with an intra-oceanic setting for the basalt sequences (e.g. Isozaki et al., 1990; Buslov et al., 2001; Dobretsov et al., 2004; Safonova et al., 2004, 2008; Figs. 12, 13c, d). Compared to typical crustally contaminated IAB and BAB the Agardag basalts are characterized by higher Nb and lower Th concentrations resulting in less “deep” Nb anomalies on the multi-component diagrams and, in average, possess generally higher levels of trace-element concentrations (Fig. 12a, g). Thus, we reject significant crustal contamination of the given basaltic lavas because: 1) Nb/La<sub>pm</sub> ratios do not correlate with Th/La<sub>pm</sub>; 2) the observed Nb minimums relative to Th and La are much less pronounced than those of IAB and BAB (Fig. 12); 3) geology–lithological relationships show that the basaltic units formed over the oceanic, not continental, lithosphere; and 4) Nb and Th concentrations for a part of basaltic samples were obtained by XRF, which may yield rather high analytical errors on these two elements (up to 20–30%), and needs to be further analyzed. The low Nb/La<sub>pm</sub> values in some basalts possibly resulted not from contamination of mafic melts by continental crust material during eruption (exogenous contamination), but from recycling of lithosphere into the mantle during subduction of the oceanic slab (endogenous contamination; Polat et al., 1999). The relatively low concentrations of Th, most data within the range 2–5 ppm fitting the average OIB of Sun and McDonough (1989), also rule out crustal contamination (Table 3). Although, several samples of the Kurai, and Akiyoshi ACs plot below the Nb/Th<sub>pm</sub> = 1 line (Fig. 13c, d) these basalts display much less Th enrichment, i.e. Th/Nb<sub>pm</sub> < La/Nb<sub>pm</sub> or Nb/La<sub>pm</sub> > Th/La<sub>pm</sub>, compared to most suprasubduction basalts and BAB, which are characterized by Th/Nb<sub>pm</sub> > 2.

### 5.3. Specific geochemical features and mantle sources of intraplate basalts

Geochemical features of volcanic rocks are important for assessing the geodynamic environment of their formation and the type of mantle source. In our case most basaltic lavas, except for those from Mongolia, have been formerly proved to form in an oceanic island setting (see references in Tables 2–4). Similarly to typical OIBs, the plume-related basalts of the PAO and PPO are usually characterized by medium to high TiO<sub>2</sub> (> 1.5 wt.%), medium to high LREE (La/Sm<sub>n</sub> > 1.3), differentiated HREE (Gd/Yb<sub>n</sub> > 1.4) and elevated Nb contents (Nb<sub>av.</sub> = 26.1; Nb/La<sub>pm</sub> = 1.23, Nb/Th<sub>pm</sub> = 1.71 as averages; also see Tables 3, 4; Figs. 10–13). Al<sub>2</sub>O<sub>3</sub>/TiO<sub>2</sub> ranges from 4 to 10 compared to 15–25 in IAB and BAB and 10–15 in MORB (Figs. 9 and 13a, b; Table 3). The geochemical characteristic of the Bayanhongor, Agardag, Ulaanbaatar and Solonker lavas match those geochemical criteria, although the Agardag basalts been previously regarded as back-arc basalts only (Pfander et al., 2000, 2002).

The medium to high differentiation of HREE reflects mantle melting in the garnet stability field (e.g. Hirschmann and Stolper, 1996; Fig. 11), because HREE are partly garnet compatible elements. Besides, it is a common knowledge that plume-related volcanic rocks are special for Nb enrichment (e.g. Sun and McDonough, 1989; Figs. 12 and 13). Saunders et al. (1988) supposed that Nb resides in the subducting oceanic slab, whereas LREE and Th are fractionated from it



to be transferred to the subarc mantle. Nb is an element compatible in Fe–Ti oxides only, such as rutile, which dominates the budget of incompatible elements relative to LREE in the eclogites formed during subduction (Rudnik et al., 2000). Nb can fractionate from Th and LREE through subduction-induced dehydration and accumulate through the mixing of subducted oceanic slabs back into the lower mantle, possibly reaching the core–mantle boundary (McCulloch and Gamble, 1991; Brenan et al., 1994). Another “deep-mantle signature” of basaltic melt sources is Zr (Hf) anomalies present in many trace-element diagrams (Fig. 12) and also suggesting deep melt segregation of plume-related basaltic liquids with majorite garnet at depths of >400 km (Xie et al., 1993).

Thus, high Gd/Yb<sub>n</sub>, Nb/Th<sub>pm</sub>, Nb/La<sub>pm</sub> ratios and negative Zr anomalies present on the trace-element multi-component diagrams (Figs. 11 and 12) suggest a lower mantle source of incompatible elements and deep mantle melting within the garnet stability field in a mantle plume column.

However, the mantle plume column may be heterogeneous and contain mixed enriched and depleted melts resulting in variable enrichment in incompatible elements, such as Ti, REE, Nb and Th (e.g., Silver et al., 1988; Mahoney et al., 1993; Hards et al., 1995). The degree of such enrichment probably depends on the degree of partial melting (Regelous et al., 2003 and references therein). Younger seamounts formed over thinner oceanic lithosphere and/or close to mid-oceanic ridge spreading zones (Regelous et al., 2003; Safonova, 2008) may have lower concentrations of Nb and negative Nb anomalies compared to typical OIB (Figs. 11g, 12g). However, unlike surpsubduction basalts, they are characterized by Nb/Th<sub>pm</sub> < Nb/La<sub>pm</sub> (Figs. 11 and 13c, d). Those lavas, like the older seamounts of the Emperor Seamount Chain (Meiji, Detroit), possess flatter REE patterns, which are indicative of shallower depth and/or higher degrees of melting (e.g. Hofmann, 1997; Polat et al., 1999; Regelous et al., 2003; Table 3; Fig. 11). Near-flat HREE patterns of the Kurai basalts are furthermore consistent with a shallower melting depth (Safonova, 2008), although the majority of basaltic units from PAO and PPO accretionary complexes are dominated by lavas with trace-element enriched signatures (high La/Sm<sub>n</sub>, Gd/Yb<sub>n</sub> and low Zr/Nb; Fig. 11, Tables 3, 4).

#### 5.4. Problems of identification of intraplate basalts

Identification of plume-related basalts in accretionary complexes seems to be of special importance because in past decades such complexes were sometimes erroneously regarded as island-arc or back-arc basalts or ophiolites (MORB). Now it is possible to differentiate those basalts due to more precise determination of trace-element and isotopic ratios, mainly based on inter-element relationships in the LREE–Th–Nb system, and taking into account their associated sedimentary rocks.

Ti–LREE–Nb-enriched basalts associated with OPS sediments have been sporadically mentioned in many island-back-fore-arc and ophiolitic terranes, however, they are often regarded as an integral part of the terrane. Several publications regarding the Lake (“Ozyornaya” in Russian) island-arc (Kovalenko et al., 1996), Agardag back-arc (Pfander et al., 2002) or Bayanhongor ophiolitic terranes of Mongolia (Kovalenko et al., 2005) show geochemical data sheets including several (2–5) basalt compositions having mantle plume signatures, however they have not been paid special attention and have been interpreted as plume-related lavas. For example, the selected Agardag basalts have OIB-type REE patterns (Fig. 11a), trace-element patterns partly similar to OIB and clearly different from IAB and BAB (Fig. 12a, g) and Al<sub>2</sub>O<sub>3</sub>/TiO<sub>2</sub> and Nb/Th<sub>pm</sub> ratios different from those typical for IAB (Fig. 13a, c). The reason for such misinterpretation may be the occasional sampling of such units which are mixed in outcrops with island-arc formations, OPS units and tectonic mixtites. Those units, as a rule, significantly exceed OIB-type lavas in volume. The area of the Kuznetsk–Altai island-arc units in Russian Altai, for instance, is ten

times larger than that total of the Kurai and Katun accretionary complexes (Fig. 3). Therefore structurally complicated island-arc and accretionary complexes require a special, very detailed field study and sampling with a special emphasis on the occurrence of sedimentary OPS units such as massive limestone, carbonate breccia, synsedimentary folded epiclastic sediments, radiolarian/ribbon chert. We believe that many island-back-fore-arc terranes, which presently occur within intracontinental foldbelts and include accretionary complexes, may host smaller fragments, tectonically separated blocks or sheets, of former oceanic islands/seamounts and their identification is just a matter of future study (see Section 5.5).

#### 5.5. Future study of intraplate basalts

Recognizing oceanic basalts of intraplate origin – oceanic islands, seamounts and plateaus – as elements of Oceanic Plate Stratigraphy is necessary for reconstructing the evolution of paleo-oceans from their opening, recorded in riftogenic dikes of OIB-type basalts, through the maximal opening, recorded in intraplate OPS units, finally to their closure, recorded in accretionary complexes. The study of intraplate magmatism and OPS is also very important because it is an integral part of the study of orogenic belts incorporating many commercially valuable mineral deposits. Finally, identification of OIB is important for mantle plume modeling and global geodynamic paleoreconstructions.

On the other hand, the study of intraplate formations is important in terms of continental growth. Since oceanic rises are typically thicker and more buoyant than the oceanic crust formed at mid-oceanic ridges, they reinforce accretion of oceanic material to the continental margins. Therefore, the accretion of plume-related oceanic islands, seamounts and plateaus during convergence of plates probably played an important role in the growth of the continental crust since the beginning of the plate tectonics (e.g. Stein and Hofmann, 1994; Albarede, 1998).

Many regions located within giant folded areas such as the Central Asian Orogenic Belt remain insufficiently studied on this topic. The Middle Ordovician–Middle Devonian gap in the PAO intraplate magmatism, which was discussed in Safonova (2009), may be partly filled by the first data on the Ulaanbaatar AC (see Section 2.3; Fig. 4) and very limited information about the Kokshaal AC in Central Tien Shan (Kyrgyzstan) hosting Late Ordovician–Silurian (?) oceanic sediments associated with basalts possessing plume-type geochemical features, however, most papers on this region present no table data sheets (Biske and Tabuns, 1996; Burtman, 2007). No detailed study of these basalts and their relationships with the sediments in terms of the OPS model has ever been performed. Yakubchuk (pers. comm.) commented that high-Ti basalts occur in accretionary complexes in Central Kazakhstan, which also may include Ordovician–Devonian OPS units, but so far no detailed geochemical data on OIB-type basalts and/or biostratigraphically dated OPS units have also been reported.

If we identify and prove the occurrence of Middle Paleozoic OPS units in Central Tien Shan (Kokshaal AC), Central Kazakhstan (?) and northern Mongolia (Ulaanbaatar AC), we would confirm the continuous character of the intraplate magmatism of the Paleo-Asian Ocean, like that of the Paleo-Pacific Ocean, which started in the Late Paleozoic and is still continuing on the Hawaii islands. The Late Cretaceous OIB-type lavas (Smagin AC) of probably the oldest part of the Emperor-Hawaii Seamount Chain link the Paleo-Mesozoic intraplate magmatism of the Paleo-Pacific Ocean and the Cenozoic intraplate magmatism of the Pacific Ocean.

In terms of possible misinterpretation of plume-related oceanic basalts presently regarded as parts of island-arc and back-arc terranes, a more careful study should be performed in the Agardag, Bayanhongor and Lake terranes in Mongolia. A limited amount of good-quality trace-element data (Table 4) is available on the geologically well

studied Bayahhongor, Samarka, Taukha and Southern Chichibu ACs. Almost no geochemical data have been reported for the basalts of the Ulaanbaatar and Khabarovsk ACs. Thus, more careful field study and sampling is necessary in these areas in order to obtain good quality geochemical data on the OIB-type basalts, especially ICP MS trace-element data.

Further potential for the study of mantle plume magmatism lies in tracing the temporal geochemical evolution of trace-element and isotope compositions of plume-related lavas. Such a problem can be regarded from a local and global point of view. The “local” approach implies the study of basalts, which were erupted over one hot spot within one oceanic plate, i.e. within the lifetime of an oceanic plate. The trace-element and isotope composition of intraplate basalts can vary with the age of the underlying oceanic lithosphere at the time of seamount magmatism due to variable degrees of melting of a heterogeneous mantle related to variable lithosphere thickness. Such a tendency was previously shown for the Emperor-Hawaiian Seamount Chain (Regelous et al., 2003) and Late-Neoproterozoic–Cambrian lavas of the PAO (Safonova, 2008). Thus, special attention should be paid to the basalts which were probably formed over the same oceanic plate, for example, the Akiyoshi and/or Mino-Tamba basalts of different ages (Carboniferous to Permian). According to the paleoreconstructions of Maruyama et al. (1997) these basalts probably formed over the Farallon and Izanagi plate, respectively. However, to use such an approach we need biostratigraphically well-dated basaltic units, representative sets of good quality trace-element and isotopic data for each OPS-basalt unit and reliable geodynamic paleoreconstructions for each age group of units for a given paleo-ocean.

The “global” approach implies a general comparison of different geochemical types of OIB-type basalts (e.g. incompatible element enriched and non-enriched varieties) of different ages, for example, for a period from the Late Neoproterozoic to the Quaternary. However, a lack of available/reliable geochemical data prevents a solution to this problem. The amount of good-quality trace-element data is insufficient for some units, in particular, for the ACs of Mongolia and Russian Far East; moreover, the isotope data are still unavailable for most basaltic units under consideration except for the Akiyoshi and Mino-Tamba AC of Japan (Sano et al., 2000; Ichiyama et al., 2008, respectively) and only limited data on the Kurai and Katun ACs in Russian Altai (Safonova, 2008). Thus, the problem of tracing the temporal geochemical evolution of OIBs is very important for geodynamic and petrologic modeling of Paleo-Asian Ocean and Paleo-Pacific Ocean intraplate magmatism, but requires further research.

## 6. Conclusions

The plume-related oceanic basalts presently hosted by accretionary complexes of Russian Altai, East Kazakhstan, Mongolia, Russian Far East (including Kamchatka) and Japan were formed in the Paleo-Asian and Paleo-Pacific oceanic realms in relation to the Pacific Superplume. The intraplate magmatism started during the Late Neoproterozoic in the Paleo-Asian Ocean and continued until the Late Cretaceous in the Paleo-Pacific Ocean. The intraplate basalts, together with sedimentary units of oceanic plate stratigraphy, were later accreted to active continental margins during oceanic plate subduction.

In spite of different ages the basalts have much in common: a similar geological position in accretionary complexes of orogenic belts formed during closure of paleo-oceans and subsequent collisional processes, spatial relation to mélange zones and island-arc formations, and their close association with OPS units, which are indicative of their formation on an oceanic rise: reefal limestone, carbonate breccia and other slope facies, hemipelagic siliceous shale, pelagic chert.

The majority of samples considered in this study possess geochemical affinities of typical OIB basalts formed in an intraplate

oceanic setting: medium to high  $\text{TiO}_2$  (>1.5 wt.%), enriched LREE ( $\text{La}/\text{Sm}_n > 1.3$ ), differentiated HREE ( $\text{Gd}/\text{Yb}_n > 1.4$ ), and elevated Nb contents ( $\text{Nb}_{\text{av}} = 26.1$ ) resulting in positive Nb anomalies relative to Th and La on the trace-element diagrams ( $\text{Nb}/\text{La}_{\text{pm}} = 1.2\text{--}1.9$ ;  $\text{Nb}/\text{Th}_{\text{pm}} = 1.02\text{--}5.6$ ). The paper presented first geochemical data on the Middle Paleozoic intraplate basalts of the Ulaanbaatar AC in Northern Mongolia, which partly filled the Middle Ordovician–Middle Devonian gap in the Paleo-Asian Ocean plume-related magmatism.

The intraplate magmatism of both oceans was continuous, with a probable periodicity of about 50 Ma. The successive character of the PAO magmatism can be more reliably proven by the careful study of the Silurian to Devonian OPS units including intraplate basalts in Mongolia and Kyrgyzstan (Central Tien Shan).

More sampling seems to be necessary in the island-arc and back-arc terranes of Mongolia and NE China (e.g. Lake, Agardag, Solonker) for re-identification of intraplate basalts and also in the Ulaanbaatar (Mongolia), Southern Chichibu (Japan), Khabarovsk and Taukha (Russian Far East) accretionary complexes for obtaining new, good quality geochemical data.

## Acknowledgements

Inna Safonova would like to express her cordial thanks to Drs. Mikhail Buslov (IGM SB RAS) and Tsutomu Ota (Okayama University) for many years of joint fieldwork and to Prof. Maruyama for permanent support and encouragement during the research. The authors thank Dr. Clare Davies (Woodside Energy Ltd., Australia) for editing the English of the manuscript and Dr. Dmitry Saveliev (ISV DVO RAS) for providing samples of the Smagin paleoseamount. Prof. Andrei Izokh (IGM SB RAS) and Dr. Igor Kemkin (FEGI DVO RAS) are greatly appreciated for sharing analyses on the Katun seamount and Taukha/Samarka ACs, respectively. The reviews by an anonymous reviewer and Prof. Dilek substantially improved the manuscript. The work was supported by RFBF-JSPS international grant no. 07-05-91211a.

## Appendix A. Supplementary data

Supplementary data associated with this article can be found, in the online version, at [doi:10.1016/j.gr.2009.02.008](https://doi.org/10.1016/j.gr.2009.02.008).

## References

- Albarede, F., 1998. The growth of continental crust. *Tectonophysics* 296, 1–14.
- Badarch, G., Cunningham, W.D., Windley, B.F., 2002. A new terrane subdivision for Mongolia: implications for the Phanerozoic crustal growth of Central Asia. *Journal of Asian Earth Sciences* 21, 87–110.
- Belyanskiy, G.S., Nikitina, A.P., Rudenko, V.S., 1984. The Sebuchar Suite in Primorje. In: Poyarkova, Z.N. (Ed.), *New Data on the Phanerozoic Biostratigraphy of Far East*. Far East Scientific Center of the USSR Academy of Science (DVNC AN SSSR) Publ., Vladivostok, pp. 43–57 (in Russian).
- Biske, Yu.S., Tabuns, E.V., 1996. Atbashi–Kokshaal Hercynides, Central Tien Shan: precollisional stage basalts and their geodynamic nature. *Doklady Earth Sciences* 348, 540–545.
- Bragin, N.Yu., 1992. Stratigraphy of Upper Paleozoic and Mesozoic units near Khabarovsk. *Izvestiya Akademii Nauk SSSR. seria geologicheskaya*, vol. 2, pp. 35–40 (in Russian).
- Brenan, J.M., Shaw, H.F., Phinney, D.L., Ryerson, F.J., 1994. Rutile–aqueous fluid partitioning of Nb, Ta, Hf, Zr, U and Th: implications for high-field strength element depletions in islandarc basalts. *Earth and Planetary Science Letters* 128, 327–339.
- Burtman, V.S., 2007. Tien Shan and High Asia: Paleozoic Tectonics and Geodynamics. *GEOS, Moscow*, p. 214 (in Russian).
- Buslov, M.M., Berzin, N.A., Dobretsov, N.L., Simonov, V.A., 1993. *Geology and tectonics of Gorny Altai*. UIGGM, Novosibirsk, p. 122.
- Buslov, M.M., Fujiwara, Y., Safonova, I.Yu., Okada, S.H., Semakov, N.N., 2000. The junction zone of the Gorny Altai and Rudny Altai terranes: structure and evolution. *Russian Geology and Geophysics* 41, 377–390.
- Buslov, M.M., Safonova, I.Yu., Watanabe, T., Obut, O., Fujiwara, Y., Iwata, K., Semakov, N.N., Sugai, Y., Smirmova, L.V., Kazansky, A.Yu., 2001. Evolution of the Paleo-Asian Ocean (Altai–Sayan region, Central Asia) and collision of possible Gondwana-derived terranes with the southern marginal part of the Siberian continent. *Geosciences Journal* 5, 203–224.

- Buslov, M.M., Fujiwara, Y., Iwata, K., Semakov, N.N., 2004a. Late Paleozoic–Early Mesozoic geodynamics of Central Asia. *Gondwana Research* 7, 791–808.
- Buslov, M.M., Watanabe, T., Fujiwara, Y., Iwata, K., Smirnova, L.V., Safonova, I.Yu., Semakov, N.N., Kiryanova, A.P., 2004b. Late Paleozoic faults of the Altai region, Central Asia: tectonic pattern and model of formation. *Journal of Asian Earth Sciences* 23, 655–671.
- Chen, C.-Y., Frey, F.A., Garcia, M.O., Dalrymple, G.B., Hart, S.R., 1991. The tholeiitic to alkaline basalt transition at Heleakala volcano. Maui, Hawaii. *Contributions to Mineralogy and Petrology* 106, 183–200.
- Condie, K.C., 2003. Supercontinents, superplumes and continental growth: the Neoproterozoic record. In: Yoshida, M., Windley, B.F., Dasgupta, S. (Eds.), *Proterozoic East Gondwana: Super Continent Assembly and Break-up*. Special Publication, vol. 206. Geological Society, London, pp. 1–21.
- Coticelli, A., Guarnieri, L., Farinelli, A., Mattei, M., Avanzinelli, R., Bianchini, G., Boari, E., Tommasini, S., Tiepolo, M., Prelevic, D., Venturelli, G., 2009. Trace elements and Sr–Nd–Pb isotopes of K-rich, shoshonitic, and calc-alkaline magmatism of the Western Mediterranean Region: genesis of ultrapotassic to calc-alkaline magmatic association in a post-collisional geodynamic setting. *Lithos* 107, 68–92.
- Dalziel, I.W.D., 1992. Antarctica: a tale of two supercontinents. *Annual Reviews in Earth and Planetary Sciences* 20, 501–526.
- Dampare, S.B., Shibata, T., Asiedu, D.K., Osae, S., Banoeng-Yakubo, B., 2008. Geochemistry of Paleoproterozoic metavolcanic rocks from the southern Ashanti volcanic belt, Ghana: petrogenetic and tectonic setting implications. *Precambrian Research* 162, 403–423.
- Dobretsov, N.L., Watanabe, T., Natal'in, B., Miyashita, S., 1994. Comparison of ophiolites and blueschists of Sakhalin and Hokkaido. *Ophiolite* 19, 157–176.
- Dobretsov, N.L., Berzin, N.A., Buslov, M.M., 1995. Opening and tectonic evolution of the Paleo-Asian Ocean. *International Geology Review* 37, 335–360.
- Dobretsov, N.L., Buslov, M.M., Vernikovskiy, V.A., 2003. Neoproterozoic to Early Ordovician evolution of the Paleo-Asian Ocean: implications to the break-up of Rodinia. *Gondwana Research* 6, 143–159.
- Dobretsov, N.L., Buslov, M.M., Safonova, I.Yu., Kokh, D.A., 2004. Fragments of oceanic islands in the Kurai and Katun' accretionary wedges of Gorniy Altai. *Russian Geology and Geophysics* 45, 1381–1403.
- Dobretsov, N.L., Kiryashkin, A.G., Kiryashkin, A.A., 2005. Parameters of hot spots and thermochemical plumes. *Russian Geology and Geophysics* 46, 575–589.
- Golozubov, V.V., Khanchuk, A.I., Kemkin, I.V., Panchenko, I.V., Simanenko, V.P., 1992. *Taukha and Zhuravlev Terranes of the Southern Sikhote-Alin*. Far-East Geological Institute Publishing House, Vladivostok, p. 82 (in Russian).
- Hara, H., Wakita, K., Ueno, K., Kamata, Y., Hisada, K., Charusiri, P., Charoentitrat, T., Chaodumrong, P., 2009. Nature of accretion related to Paleo-Tethys subduction recorded in northern Thailand: constraints from mélange kinematics and illite crystallinity. *Gondwana Research* 16 (2), 310–320.
- Hards, V.L., Kempton, P.D., Thompson, R.N., 1995. The heterogeneous Iceland plume: new insights from the alkaline basalts of the Snaefell volcanic centre. *Journal of the Geological Society* 152, 1003–1009.
- Hirschmann, M.M., Stolper, E.M., 1996. A possible role for garnet pyroxenite in the origin of the "garnet signature" in MORB. *Contributions to Mineralogy and Petrology* 124, 185–208.
- Hofmann, A.W., 1997. Mantle geochemistry: the message from oceanic volcanism. *Nature* 385, 219–229.
- Humphris, S.E., 1984. The mobility of the rare earth elements in the crust. In: Henderson, P. (Ed.), *Rare Earth Element Geochemistry*. Elsevier, Amsterdam, pp. 317–342.
- Ichiyama, Y., Ishiwatari, A., Koizumi, K., 2008. Petrogenesis of greenstones from the Mino-Tamba belt, SW Japan: evidence for an accreted Permian oceanic plateau. *Lithos* 100, 127–146.
- Ishiwatari, A., Nakae, S., 2001. Yakuno ophiolite and greenstones of the Tamba belt in the Wakasa areas, Fukui prefecture. *Excursion Guidebook, the 108th Annual Meeting, Geological Society of Japan, Kanazawa*, pp. 67–84.
- Isozaki, Y., 1997. Contrasting two types of orogens in Permo-Triassic Japan: accretionary versus collisional. *Island Arc* 6, 2–24.
- Isozaki, Y., Maruyama, Sh., Fukuoaka, F., 1990. Accreted oceanic materials in Japan. *Tectonophysics* 181, 179–205.
- Iwata, K., Obut, O.T., Buslov, M.M., 1997a. Devonian and Lower Carboniferous radiolaria from the Chara ophiolite belt, East Kazakhstan. *News of Osaka Micropaleontologist* 10, 27–32.
- Iwata, K., Sennikov, N.V., Buslov, M.M., Obut, O.T., Shokalsky, S.P., Kuznetsov, S.A., Ermikov, V.D., 1997b. Upper Cambrian–Early Ordovician age of the Zalur'ia basalt–chert–terigenous formation (northwestern Gorniy Altai). *Russian Geology and Geophysics* 38, 1427–1444.
- Jenner, G.A., Longerich, H.P., Jackson, S.E., Fryer, B.J., 1990. ICP-MS – a powerful tool for high precision trace element analysis in earth sciences: evidence from analysis of selected U.S.G.S. reference samples. *Chemical Geology* 83, 133–148.
- Joplin, G.A., Kiss, E., Ware, N.G., Widdowson, J.R., 1972. Some chemical data on members of the shoshonite association. *Mineralogical Magazine* 38, 936–945.
- Kanmera, K., Sano, H., Isozaki, Y., 1990. Akiyoshi terrane. In: Ichikawa, K., Mizutani, S., Hara, I., Hada, S., Yao, A. (Eds.), *Pre-Cretaceous Terranes of Japan*. Publication of IGCP Project: Pre-Jurassic Evolution of Eastern Asia No. 224, Osaka, pp. 49–62.
- Kashiwagi, K., Tsukada, K., Minjin, B.C., 2004. Paleozoic spherical radiolarians from the Gorkhi Formation, southwest Khentii range, central Mongolia; a preliminary report. *Mongolian Geoscientist* 24, 17–26.
- Kemkin, I.V., 2006. The Mesozoic Geodynamic Evolution of the Sikhote-Alin and Japan Sea Region. *Nauka, Moscow*, p. 258 (in Russian).
- Kepezhinskas, P.K., Kepezhinskas, K.B., Puchtel, I.S., 1991. Lower Paleozoic oceanic crust in Mongolian Caledonides: Sm–Nd isotope and trace element data. *Geophysical Research Letters* 18, 1301–1304.
- Kerr, A.C., 1998. Oceanic plateau formation: a cause of mass extinction and black shale deposition around the Cenomanian–Turonian boundary? *Journal of the Geological Society of London* 155, 619–626.
- Khanchuk, A.I., Kemkin, I.V., 2003. Mesozoic geodynamic evolution of the Japan Sea Region. *Vestnik DVO RAN* 6, 94–108 (in Russian).
- Khanchuk, A.I., Kemkin, I.V., Panchenko, I.V., 1989a. Geodynamic evolution of Sikhote-Alin and Sakhalin in Middle Paleozoic and Early Mesozoic. In: Scheglov, A.D. (Ed.), *Pacific Margin of Asia: Geology*. Nauka, Moscow, pp. 218–255 (in Russian).
- Khanchuk, A.I., Nikitina, A.P., Panchenko, I.V., Buriy, G.I., Kemkin, I.V., 1989b. Paleozoic and Mesozoic guyots of Sikhote-Alin and Sakhalin. *Doklady Akademii Nauk SSSR* 307, 186–190.
- Khotin, M., Shapiro, M., 2006. Ophiolites of the Kamchatsky Mys Peninsula, eastern Kamchatka: structure, composition, and geodynamic setting. *Geotectonics* 40, 297–320.
- Kimura, G., Sakakibara, M., Okamura, M., 1994. Plumes in central Panthalassa? Deductions from accreted oceanic fragments in Japan. *Tectonics* 13, 905–906.
- Koizumi, K., Ishiwatari, A., 2006. Oceanic plateau accretion inferred from Late Paleozoic greenstones in the Jurassic Tamba accretionary complex, southwest Japan. *Island Arc* 15, 58–83.
- Kojima, S., Kemkin, I.V., Kametaka, M., Ando, A., 2000. A correlation of accretionary complexes of southern Sikhote-Alin of Russia and the Inner zone of southern Japan. *Geoscience Journal* 4, 175–185.
- Komiya, T., Maruyama, Sh., Hirata, T., Yurimoto, H., Nohda, S., 2004. Geochemistry of the oldest MORB and OIB in the Isua Supracrustal Belt, Southern West Greenland implication for the composition and temperature of early Archaean upper mantle. *The Island Arc* 13, 47–72.
- Kopteva, V.V., Kuzmin, M.I., Tomurtogoo, O., 1984. The structure of the upper part of the Bayanhongor ophiolites, Mongolia. *Geotectonics* 6, 39–54 (in Russian).
- Kovach, V.P., Jian, P., Yarmolyuk, V.V., Kozakov, I.K., Liu, D., Terent'eva, L.B., Lebedev, V.I., Kovalenko, V.I., 2005. Magmatism and geodynamics of early stages of the Paleozoic Ocean formation: geochronological and geochemical data on ophiolites of the Bayanhongor Zone. *Doklady Earth Sciences* 404, 1072–1077.
- Kovalenko, V.I., Yarmolyuk, V.V., Pukhtel, I.S., Stosch, H., Jagoutz, E., Korikovskiy, S.P., 1996. Magmatic rocks and magma sources of ophiolites of the Lake zone, Mongolia. *Petrology* 4, 453–495 (in Russian).
- Kovalenko, V.I., Yarmolyuk, V.V., Tomurtogoo, O., Antipin, V.S., Kovach, V.P., Kotov, A.B., Kudryashova, E.A., Sal'nikova, E.B., Zagornaya, N.Yu., 2005. Geodynamics and crust-forming processes in the Early Caldeonides of the Bayanhongor zone, Central Mongolia. *Geotectonics* 4, 55–76.
- Kurenkov, S.A., Didenko, A.N., Simonov, V.A., 2002. Geodynamics of Paleospreading. *GEOS, Moscow*, p. 294 (in Russian).
- Kurihara, T., Tsukada, K., Otoh, S., Kashiwagi, K., Minjin, Ch., Sersmaa, G., Dorjsuren, B., Bujinlkham, B., 2006. Middle Paleozoic radiolarians from the Gorki Formation, Central Mongolia. In: Tomurhuu, D., Natal'in, B., Ariunchimeg, Y., Khishigsuren, S., Erdenesaikhan, G. (Eds.), *Structural and Tectonic Correlation Across the Central Asian Orogenic Collage: Implications for Continental Growth and Intracontinental Deformation*. IGCP Project-480 2<sup>nd</sup> Int. Workshop, Ulaanbaatar, IGMR MAS, pp. 67–68.
- Ludden, J.N., Thompson, G., 1978. Behavior of rare earth elements during submarine weathering of tholeiitic basalts. *Nature* 274, 147–149.
- Manya, S., Maboko, M.A.H., 2008. Geochemistry and geochronology of Neoproterozoic volcanic rocks of the Iramba–Sekenke greenstone belt, central Tanzania. *Precambrian Res* 163 (3–4), 265–278.
- Mahoney, J.J., Storey, M., Duncan, R.A., Spencer, K.J., Pringle, M., 1993. Geochemistry and geochronology of Leg130 basement lavas: nature and origin of the Ontong Java Plateau. *Proceedings of the Ocean Drilling Program. Scientific Results*, vol. 130, pp. 3–22.
- Maruyama, S., 1994. Plume tectonics. *Journal of Geological Society of Japan*, 100, 24–49.
- Maruyama, S., Isozaki, Y., Kimura, G., Terabayashi, M., 1997. Paleogeographic maps of the Japanese Islands: plate tectonic synthesis from 750 Ma to the present. *Island Arc* 6, 121–142.
- Maruyama, S., Santosh, M., Zhao, D., 2007. Superplume, supercontinent, and post-perovskite: mantle dynamics and anti-plate tectonics on the Core–Mantle Boundary. *Gondwana Research* 11, 7–37.
- Matsuoka, A., Yao, A., 1990. Southern Chichibu Terrane. In: Ichikawa, K., Mizutani, Sh., Hara, I., Hada, Sh., Yao, A. (Eds.), *Publication of IGCP Project: Pre-Jurassic Evolution of Eastern Asia No. 224*, Osaka. Pre-Cretaceous Terranes of Japan, pp. 203–216.
- McCulloch, M.T., Gamble, A.J., 1991. Geochemical and geodynamical constraints on subduction zone magmatism. *Earth and Planetary Science Letters* 102, 358–374.
- McDonough, W.F., Sun, S.-S., 1995. The composition of the Earth. *Chemical Geology* 120, 223–253.
- Medvedev, A.Y., Al'Mukhamedov, A.I., Kirda, N.P., 2003. Geochemistry of Permo-Triassic volcanic rocks of West Siberia. *Russian Geology and Geophysics* 44, 86–100.
- Miao, L., Fan, W., Liu, D., Zhang, F., Shi, Yu., Gu, F., 2008. Geochronology and geochemistry of the Hegenshan ophiolite complex: implications for late-stage tectonic evolution of the Inner Mongolia–Daxinganling Orogenic Belt, China. *Journal of Asian Earth Sciences* 32, 348–370.
- Minjin, C., Tomurtogoo, O., Dorjsuren, B., 2006. Excursion around Ulaanbaatar. In: Tomurhuu, D., Natal'in, B., Ariunchimeg, Y., Khishigsuren, S., Erdenesaikhan, G. (Eds.), *Structural and Tectonic Correlation across the Central Asian Orogenic Collage: implications for Continental Growth and Intracontinental Deformation*. IGCP Project-480 2<sup>nd</sup> Int. Workshop Abstracts and Excursion Guidebook, Ulaanbaatar, IGMR MAS, pp. 99–106.
- Nakae, S., 2000. Regional Correlation of the Jurassic Accretionary Complex in the Inner Zone of Southwest Japan. *Memories of Geological Society of Japan*, vol. 55, pp. 73–98 (in Japanese with English abstract).
- Neal, C.R., Mahoney, J.J., Kroenke, L.W., Petterson, M.G., 1997. The Ontong Java Plateau. In: Mahoney, J.J. (Ed.), *Large Igneous Provinces: Continental, Oceanic and*



- Planetary Flood Volcanism. Geophysical Monograph. American Geophysical Union, pp. 183–216.
- Nesbitt, H.W., Young, G.M., 1982. Early Proterozoic climates and plate motions inferred from major element chemistry of lites. *Nature* 299, 715–717.
- Onoue, T., Nagai, K., Kamishima, A., Seno, M., Sano, H., 2004. Origin of basalts from Sambosan accretionary complex, Shikoku and Kyushu. *Journal of Geological Society of Japan* 110, 222–236.
- Ota, T., Utsunomiya, A., Uchio, Yu., Isozaki, Y., Buslov, M., Ishikawa, A., Maruyama, Sh., Kitajima, K., Kaneko, Y., Yamamoto, H., Katayama, I., 2007. Geology of the Gorny Altai subduction–accretion complex, southern Siberia: tectonic evolution of a Vendian–Cambrian intra-oceanic arc. *Journal of Asian Earth Sciences*, 30, 666–695.
- Parfenov, L.M., Bulgatov, A.N., Gordienko, I.V., 1995. Terranes and accretionary history of the Transbaikalian orogenic belts. *International Geology Review* 37, 736–751.
- Parfenov, L.M., Khanchuk, A.I., Badarch, G., Miller, R.J., Naumova, V.V., Nokleberg, W.J., Ogasawara, M., Prokopyev, A.V., Yan, H., 2006. North-East Asia Geodynamic Map. <http://pubs.usgs.gov/of/2006/geopubs.wr.usgs.gov/open-file/of03-205/>.
- Pavlova, E.E., Manankov, I.N., Morozova, I.P., Solovjeva, M.N., Suetenko, O.D., Bogoslavskaya, M.F., 1991. Permian invertebrates of Southern Mongolia. *Transactions*, vol. 40. Nauka, Moscow, p. 173.
- Pfander, J.A., Jochum, K.P., Kroner, A., Kozakov, I., Oidup, C., Todt, W., 1998. Age and geochemical evolution of an early Cambrian ophiolite–island arc system in Tuva, South Central Asia. *Generation and Emplacement of Ophiolites Through Time*. Geological Survey of Finland, Special Paper, 26, p. 42.
- Pfander, J.A., Kroner, A., Jochum, K.P., Kozakov, I., Oidup, C., 2000. Ocean crust formation and crustal accretion in south-central Asia: Neoproterozoic to Early Paleozoic ophiolite and island arc systems in Tuva. In: Badarch, G., Jahn, B.-M. (Eds.), *IGCP-420. Continental Growth in the Phanerozoic: Evidence from Central Asia*. Abstracts and Excursion Guidebook Geosciences, Rennes, pp. 63–64.
- Pfander, J.A., Jochum, K.P., Kozakov, I., Kroner, A., Todt, W., 2002. Coupled evolution of back-arc and island arc-like mafic crust in the late-Neoproterozoic Agardagh Teschem ophiolite, Central Asia: evidence from trace element and Sr–Nd–Pb isotope data. *Contributions to Mineralogy and Petrology* 143, 154–174.
- Pheodorin, M.A., Bobrov, V.A., Chebykin, E.P., Goldberg, E.L., Melgunov, M.S., Filippova, S.V., Zolotarev, K.V., 2000. Comparison of synchrotron radiation X-ray fluorescence with conventional techniques for the analysis of sedimentary samples. *Geostandards Newsletter. The Journal of Geostandards and Geoanalysis* 24, 205–216.
- Pillai, D., Ishiga, H., 1987. Discovery of Late Permian radiolarians from Kozuki Formation, Kozuki–Tatsuno belt, Southwest Japan. *Journal of Geological Society of Japan* 93, 847–849.
- Polat, A., Kerrich, R., Wyman, D., 1999. Geochemical diversity in oceanic komatiites and basalts from the late Archean Wawa greenstone belts, Superior Province, Canada: trace element and Nd isotope evidence for a heterogeneous mantle. *Precambrian Research* 94, 139–173.
- Polat, A., Appel, P.W.U., Frei, R., Pan, Y., Dilek, Y., Ordonez-Calderon, J.C., Fryer, B., Hollis, J.A., Raith, J.G., 2007. Field and geochemical characteristics of the Mesoarchean (~3075 Ma) Ivisartog greenstone belt, southern West Greenland: evidence for seafloor hydrothermal alteration in supra-subduction oceanic crust. *Gondwana Research* 11, 69–91.
- Portnyagin, M.V., Savel'ev, D.P., Hoernle, K., 2005. Plume-related association of Cretaceous oceanic basalts of eastern Kamchatka: compositions of spinel and parental magmas. *Petrology* 13, 571–588.
- Rasskazov, S.V., Yasnygina, T.A., Saranina, E.V., Maslovskaya, M.N., Fefelov, N.N., Brandt, I.S., Brandt, S.B., Kovalenko, S.V., Martynuk, Yu.A., Popov, V.K., 2004. Early Cenozoic volcanism of southwestern Primorje: impulse melting of the mantle and crust. *Pacific Geology* 23, 3–31 (in Russian).
- Regelous, M., Hofmann, A.W., Abouchami, W., Galer, S.J.G., 2003. Geochemistry of lavas from the Emperor Seamounts, and the geochemical evolution of Hawaiian magmatism from 85 to 42 Ma. *Journal of Petrology* 44, 113–140.
- Reichow, M.K., Pringle, M.S., Al'Mukhamedov, A.I., Allen, M.B., Andreichev, V.L., Buslov, M.M., Davies, C.E., Fedoseev, G.S., Fitton, J.G., Inger, S., Medvedev, A.Ya., Mitchell, C., Puchkov, V.N., Safonova, I.Yu., Scott, R.A., Saunders, A.D., 2009. The timing and extent of the eruption of the Siberian Traps large igneous province: implications for the end-Permian environmental crisis. *Earth and Planetary Science Letters* 277, 9–20.
- Ren, J., Wang, Z., Chen, B., Jiang, Ch., Niu, B., Li, J., Xie, G., He, Zh., Liu, Zh., 1999. *The Tectonics of China from a Global View: a Guide to the Tectonic Map of China and Adjacent Regions*. Geological Publishing House, Beijing.
- Rudnik, R., Barth, M., Horn, I., McDonough, W.F., 2000. Rutile-bearing refractory eclogites: missing link between continents and depleted mantle. *Science* 287, 278–281.
- Ryazantsev, A.V., 1994. Ophiolites of the Bayanhongor zone in the Paleozoic structure of Mongolia. *Doklady of the Russian Academy of Sciences* 336, 651–654 (in Russian).
- Safonova, I.Yu., 2005. Vendian–Paleozoic basalts of the Paleo-Asian Ocean incorporated in foldbelts of Gorny Altai and East Kazakhstan: geodynamic settings of formation. Candidate of Sciences Thesis Autoreferate. NP AI «Geo», Novosibirsk, p. 20 (in Russian).
- Safonova, I.Yu., 2008. Geochemical evolution of the Paleo-Asian Ocean intra-plate magmatism from the Late Neoproterozoic to the Early Cambrian. *Petrology* 16, 492–511.
- Safonova, I.Yu., 2009. Intraplate magmatism and oceanic plate stratigraphy of the Paleo-Asian and Paleo-Pacific Oceans from 600 to 140 Ma. *Ore Geology Reviews* 35 (2), 137–154.
- Safonova, I.Yu., Buslov, M.M., Iwata, K., Kokh, D.A., 2004. Fragments of Vendian–Early Carboniferous oceanic crust of the Paleo-Asian Ocean in foldbelts of the Altai–Sayran region of Central Asia: geochemistry, biostratigraphy and structural setting. *Gondwana Research* 7, 771–790.
- Safonova, I.Yu., Simonov, V.A., Buslov, M.M., Ota, T., Maruyama, Sh., 2008. Neoproterozoic basalts of the Paleo-Asian Ocean (Kural accretion zone, Gorny Altai, Russia): geochemistry, petrogenesis, geodynamics. *Russian Geology and Geophysics* 49, 254–271.
- Sano, H., Kanmera, K., 1991. Collapse of ancient oceanic reef complex – what happened during collision of Akiyoshi reef complex? Sequence of collisional collapse and generation of collapse products. *Journal of Geological Society of Japan* 97, 631–644.
- Sano, H., Kojima, S., 2000. Carboniferous to Jurassic Oceanic Rocks of Mino-Tamba-Ashio Terrane, Southwest Japan. *Memories of Geological Society of Japan*, vol. 55, pp. 123–144 (in Japanese with English abstract).
- Sano, S., Hayasaka, Y., Tazaki, K., 2000. Geochemical characteristics of Carboniferous greenstones in the Inner Zine of Southwest Japan. *Island Arc* 9, 81–96.
- Santosh, M., Maruyama, S., Yamamoto, S., 2009a. The making and breaking of supercontinents: some speculations based on superplumes, super downwelling and the role of tectosphere. *Gondwana Research* 15 (3–4), 324–341.
- Santosh, M., Maruyama, S., Sato, K., 2009b. Anatomy of a Cambrian suture in Gondwana: Pacific-type orogeny in southern India? *Gondwana Research* 16 (2), 321–341.
- Saunders, A.D., Norry, M.J., Tarney, J., 1988. Origin of MORB and chemically-depleted mantle reservoirs: trace element constrains. *Journal of Petrology* 415–455 Special Lithosphere Issue.
- Saveliev, D.P., 2003. Within-plate alkali basalts of the Cretaceous accretionary complex (Eastern Kamchatka). *Volcanology and Seismology* 1, 14–20 (in Russian).
- Sennikov, N.V., Iwata, K., Ermikov, V.D., Obut, O.T., Khlebnikova, T.V., 2003. Oceanic sedimentation settings and fauna associations in the Paleozoic on the southern framing of the West Siberian Plate. *Russian Geology and Geophysics* 44, 156–171.
- Silver, P.G., Carlson, R.W., Olson, P., 1988. Deep slabs, geochemical heterogeneity, and the large-scale structure of mantle convection: investigation of an enduring paradox. *Annual Review of Earth Sciences* 16, 477–541.
- Shapiro, M.N., Soloviev, A.V., Ledneva, G.V., 2007. Is there any Relation Between the Hawaiian–Emperor Seamount Chain Bed at 43 Ma and the Evolution of the Kamchatka Continental Margin? <http://www.mantleplumes.org/Kamchatka2.html>.
- Shevelov, E.K., 1987. Age of volcanogenic–siliceous–terrigenous sediments of the basement of the Middle-Amur basin. *Pacific Geology* 3, 13–16 (in Russian).
- Stein, M., Hofmann, A.W., 1994. Mantle plumes and episodic crustal growth. *Nature* 372, 63–68.
- Sun, S., McDonough, W.F., 1989. Chemical and isotopic systematics of oceanic basalts: implications for mantle composition and processes. In: Saunders, A.D., Norry, M.J. (Eds.), *Magmatism in the Ocean Basins*. Geol. Soc. London, Special Publication, vol. 42, pp. 313–345.
- Suzuki, N., Kojima, S., Kano, H., Yamakita, S., Misaki, A., Ehiro, M., Otoh, Sh., Kurihara, T., Aoyama, M., 2005. Permian radiolarian faunas from chert in the Khabarovsk Complex, Far East Russia, and the age of each lithological unit of the Khabarovsk complex. *Journal of Paleontology* 79 (4), 686–700.
- Tatsumi, Y., Kani, T., Ishizuka, H., Maruyama, Sh., Nishimura, Yu., 2000. Activation of Pacific mantle plumes during the Carboniferous: evidence from accretionary complexes in southwest Japan. *Geology* 28, 580–582.
- Taylor, S.T., McLennan, S.M., 1985. *The Continental Crust: Composition and Evolution*. Blackwell, Oxford, 312 pp.
- Terleev, A.A., 1991. Stratigraphy of Vendian–Cambrian sediments of the Katun anticline (Gorny Altai). In: Khomentovskiy, V.V. (Ed.), *Late Precambrian and Early Paleozoic of Siberia*. UIGGM Publishing, Novosibirsk, pp. 82–106 (in Russian).
- Tomurhuu, D., Munkh-Erdene, E., 2006. Geochemical constrain on the origin of Bayanhongor ophiolite complex (Central Mongolia). In: Tomurhuu, D., Natal'in, B., Ariunchimeg, Y., Khishigsuren, S., Erdenesaikhan, G. (Eds.), *Structural and Tectonic Correlation Across the Central Asian Orogenic Collage: Implications for Continental Growth and Intracontinental Deformation*. IGCP Project-480 2nd Int., Ulaanbaatar, IGMR MAS, pp. 64–65.
- Tsukada, K., Kurihara, T., Niwa, K., Otoh, S., Hikichi, G.Y., Kashiwagi, K., Kozuka, T., Chuluun, M., Dorjsuren, B., Gonchigdorj, S., Bujinlkham, B., 2006. Geochemical feature of basalt from the Gorkhi Formation, Khangay–Khentey belt, Central Mongolia. In: Tomurhuu, D., Natal'in, B., Ariunchimeg, Y., Khishigsuren, S., Erdenesaikhan, G. (Eds.), *Structural and Tectonic Correlation Across the Central Asian Orogenic Collage: Implications for Continental Growth and Intracontinental Deformation*. IGCP Project-480 2nd Int. Workshop, Ulaanbaatar, IGMR MAS, pp. 82–83.
- Uchio, Y., Isozaki, Yu., Ota, T., Utsunomiya, A., Buslov, M., Maruyama, Sh., 2004. The oldest mid-oceanic carbonate build-up complex: setting and lithofacies of the Vendian (Late Neoproterozoic) Baratal limestone in the Gorny Altai Mountains, Siberia. *Proceedings of the Japan Academy* 80, 422–428.
- Utsunomiya, A., Ota, T., Windley, B.F., Suzuki, N., Uchio, Y., Munekata, K., Maruyama, Sh., 2007. In: Yuen, D.A., Maruyama, Sh., Karato, Sh., Windley, B.F. (Eds.), *Superplumes*. Springer, the Netherlands, pp. 363–408.
- Utsunomiya, A., Suzuki, N., Ota, T., 2008. Preserved paleo-oceanic plateaus in accretionary complexes: implications for the contributions of the Pacific superplume to global environmental change. *Gondwana Research* 14, 115–125.
- Utsunomiya, A., Jahn, B.-M., Ota, T., Safonova, I.Yu., 2009. Geochemical and Sr–Nd isotopic study of the Vendian greenstones from Gorny Altai, southern Siberia: implications for the tectonic setting of the formation of greenstones and the role of oceanic plateau in accretionary orogen. *Lithos* 113 (3–4), 443–459.
- Wang, Q., Wyman, D., Xu, J.-F., Zhao, Zh.-H., Jian, P., Xiong, X.-L., Bao, Z.-H., Li, Ch.-F., Bai, Zh.-H., 2006. Petrogenesis of Cretaceous adakitic and shoshonitic igneous rocks in the Luzong area, Anhui Province (eastern China): implications for geodynamics and Cu–Au mineralization. *Lithos* 89, 424–446.
- Weaver, B.L., 1991. The origin of ocean island basalts and member compositions: trace element and isotopic constrains. *Earth and Planetary Science Letters* 104, 381–397.
- Wignall, P.B., 2001. Large Igneous Provinces and mass extinctions. *Earth-Science Reviews* 53, 1–33.

- Winchester, J.A., Floyd, P.A., 1977. Geochemical discrimination of different magma series and their differentiation products using immobile elements. *Chemical Geology* 20, 325–343.
- Windley, B.F., Alexeiev, D., Xiao, W., Kroner, A., Badarch, G., 2007. Tectonic models for accretion of the Central Asian Orogenic Belt. *Journal of the Geological Society of London*, 164, 31–47.
- Xiao, W., Windley, B.F., Hao, J., Zhai, M., 2003. Accretion leading to collision and the Permian Solonker suture, Inner Mongolia, China: termination of the Central Asian orogenic belt. *Tectonics* 22, 1–20.
- Xie, Q., Kerrich, R., Fan, J., 1993. HFSE/REE fractionations recorded in the three komatiite–basalt sequence, Archean Abitibi belt: implications for multiple plume sources and depth. *Geochimica et Cosmochimica Acta* 57, 4111–4118.
- Yakubchuk, A.S., 2004. Architecture and mineral deposit settings of the Altaid orogenic collage: a revised model. *Journal of Asian Earth Sciences* 23, 761–779.
- Zinkevich, V.P., Kazimirov, A.D., Peive, A.A., Chumakov, G.M., 1985. New data on the tectonic structure of the Kamchatskiy Cape, Eastern Kamchatka. *Doklady AN SSSR* 285, 954–958.
- Zonenshain, L.P., Kuzmin, M.I., Natapov, L.M., 1990. *Geology of the USSR: a Plate-Tectonic Synthesis*. American Geophysical Union. Geodynamic Series, vol. 21.